

## Electronic Supplementary Information

### Chlojapolactone A, An Unprecedented 1,3-Dioxolane Linked-Lindenane Sesquiterpenoid Dimer from *Chloranthus japonicus*

Yan-qiong Guo, Gui-hua Tang, Zhen-zhen Li, Shu-ling Lin, and Sheng Yin \*

*School of Pharmaceutical Sciences, Sun Yat-sen University, Guangzhou, Guangdong  
510006, P. R. China.*

E-mail: yinsh2@mail.sysu.edu.cn; Fax: +86-20-39943090; Tel: +86-20-39943090.

#### Contents:

- S1.  $^1\text{H}$  and  $^{13}\text{C}$  NMR data for **1** in  $\text{C}_5\text{D}_5\text{N}$  and  $\text{CD}_3\text{OD}$
- S2. Experimental section
  - 2.1. General experimental procedures
  - 2.2. Plant material
  - 2.3. Extraction and isolation
  - 2.4. Semisynthesis of chloranerectuslactone V (**5**) from **3**
  - 2.5. Demonstration of the existence of compound **i** in acid-catalyzed epoxy ring-opening reaction system of **3**
  - 2.6. Nitric oxide (NO) production assays
- S3.  $^1\text{H}$  NMR (400 MHz,  $\text{CDCl}_3$ ) spectrum of chlojapolactone A (**1**)
- S4.  $^{13}\text{C}$  NMR (100 MHz,  $\text{CDCl}_3$ ) spectrum of chlojapolactone A (**1**)
- S5.  $^1\text{H}$ - $^1\text{H}$  COSY spectrum of chlojapolactone A (**1**) in  $\text{CDCl}_3$
- S6. Long rang  $^1\text{H}$ - $^1\text{H}$  COSY spectrum of chlojapolactone A (**1**) in  $\text{CDCl}_3$

- S7. HSQC spectrum of chlojapolactone A (**1**) in CDCl<sub>3</sub>
- S8. HMBC spectrum of chlojapolactone A (**1**) in CDCl<sub>3</sub>
- S9. Modified HMBC spectrum of chlojapolactone A (**1**) in CDCl<sub>3</sub>
- S10. ROESY spectrum of chlojapolactone A (**1**) in CDCl<sub>3</sub>
- S11. <sup>1</sup>H NMR (500 MHz, C<sub>5</sub>D<sub>5</sub>N) spectrum of chlojapolactone A (**1**)
- S12. <sup>13</sup>C NMR (125 MHz, C<sub>5</sub>D<sub>5</sub>N) spectrum of chlojapolactone A (**1**)
- S13. <sup>1</sup>H–<sup>1</sup>H COSY spectrum of chlojapolactone A (**1**) in C<sub>5</sub>D<sub>5</sub>N
- S14. HSQC spectrum of chlojapolactone A (**1**) in C<sub>5</sub>D<sub>5</sub>N
- S15. HMBC spectrum of chlojapolactone A (**1**) in C<sub>5</sub>D<sub>5</sub>N
- S16. <sup>1</sup>H NMR (600 MHz, CD<sub>3</sub>OD) spectrum of chlojapolactone A (**1**)
- S17. <sup>13</sup>C NMR (150 MHz, CD<sub>3</sub>OD) spectrum of chlojapolactone A (**1**)
- S18. <sup>1</sup>H–<sup>1</sup>H COSY spectrum of chlojapolactone A (**1**) in CD<sub>3</sub>OD
- S19. HSQC spectrum of chlojapolactone A (**1**) in CD<sub>3</sub>OD
- S20. HMBC spectrum of chlojapolactone A (**1**) in CD<sub>3</sub>OD
- S21. <sup>1</sup>H NMR (400 MHz, CDCl<sub>3</sub>) spectrum of **2**
- S22. <sup>13</sup>C NMR (100 MHz, CDCl<sub>3</sub>) spectrum of **2**
- S23. <sup>1</sup>H NMR (400 MHz, CDCl<sub>3</sub>) spectrum of **3**
- S24. <sup>13</sup>C NMR (100 MHz, CDCl<sub>3</sub>) spectrum of **3**
- S25. <sup>1</sup>H NMR (400 MHz, CDCl<sub>3</sub>) spectrum of **4**
- S26. <sup>13</sup>C NMR (100 MHz, CDCl<sub>3</sub>) spectrum of **4**
- S27. <sup>1</sup>H NMR (400 MHz, CDCl<sub>3</sub>) spectrum of **5**
- S28. <sup>13</sup>C NMR (100 MHz, CDCl<sub>3</sub>) spectrum of **5**
- S29. <sup>1</sup>H NMR (400 MHz, CDCl<sub>3</sub>) spectrum of intermediate **ii**
- S30. <sup>13</sup>C NMR (100 MHz, CDCl<sub>3</sub>) spectrum of intermediate **ii**
- S31. <sup>1</sup>H NMR (400 MHz, CDCl<sub>3</sub>) spectra of **8-O-methyl-i** and **8-O-methyl-4**
- S32. Chem3D molecular modeling study of **1b**
- S33. ECD spectra calculation of **1a** by TDDFT method
- 33.1. Lowest energy conformers of **1a**
- 33.2. Energy analysis table
- 33.3. Calculated ECD data
- S34. The HRESIMS data of chlojapolactone A (**1**)

S1.  $^1\text{H}$  and  $^{13}\text{C}$  NMR data for **1** in  $\text{C}_5\text{D}_5\text{N}$  and  $\text{CD}_3\text{OD}$ 

no.	<b>1<sup>a</sup></b>		<b>1<sup>b</sup></b>	
	$\delta_{\text{H}}$	$\delta_{\text{C}}$	$\delta_{\text{H}}$	$\delta_{\text{C}}$
1	1.78, m	28.4	1.73, m	28.7
2a	0.64, m	8.1	0.65, m	8.0
2b	0.71, m		0.72, m	
3	1.66, m	30.2	1.64, m	30.2
4		93.2		94.8
5	2.55, m	48.9	2.45, dd (12.7, 6.9)	49.0
6a	2.11, m	27.9	2.39, dd (16.0, 12.7)	28.1
6b	2.55, m		2.59, dd (16.0, 6.9)	
7		129.6		129.9
8		167.8		169.8
9	5.35, s	110.6	5.23, s	111.2
10		49.8		50.2
11		138.6		139.4
12		171.0		171.8
13	1.98, d (1.0)	16.6	1.97, d (1.3)	16.2
14	1.27, s	17.2	1.21, s	17.3
15	1.71, s	31.7	1.62, s	31.2
OMe	3.79, s	52.9	3.71, s	53.0
1'	1.87, m	24.7	1.86, m	24.8
2'a	0.71, m	16.3	0.72, m	16.2
2'b	0.85, m		0.90, m	
3'	2.04, m	24.4	1.99, m	24.6
4'		152.2		152.9
5'	3.61, m	51.3	3.50, m	51.8
6'a	2.31, m	22.7	2.12, dd (13.1, 13.1)	23.0
6'b	2.55, m		2.55, m	
7'		155.0		155.9
8'		110.4		111.1
9'	4.42, s	86.1	4.35, s	86.6
10'		43.4		44.0
11'		128.6		129.0
12'		171.5		172.5
13'	1.82, s	9.0	1.84, d (1.3)	8.5
14'	0.47, s	17.5	0.54, s	17.4
15'a	4.84, s	107.2	4.80, s	107.0
15'b	5.11, d (2.4)		5.02, d (2.2)	

<sup>a</sup> Recorded in  $\text{C}_5\text{D}_5\text{N}$  ( $\delta_{\text{H}}$  recorded at 400 MHz and  $\delta_{\text{C}}$  recorded at 100 MHz), <sup>b</sup> Recorded in  $\text{CD}_3\text{OD}$  ( $\delta_{\text{H}}$  recorded at 600 MHz and  $\delta_{\text{C}}$  recorded at 150 MHz), chemical shifts are in ppm, coupling constant  $J$  is in Hz.

## S2. Experimental section

### 2.1. General experimental procedures

Optical rotations were measured on a Perkin-Elmer 341 polarimeter, and CD spectra were obtained on an Applied Photophysics Chirascan spectrometer. UV spectra were recorded on a Shimadzu UV-2450 spectrophotometer. IR spectra were determined on a Bruker Tensor 37 infrared spectrophotometer with KBr disks. NMR spectra were measured on Bruker AM-400 and 600 spectrometers at 25 °C. LRESIMS was measured on a Finnigan LC Q<sup>Deca</sup> instrument, and HRESIMS was performed on a Waters Micromass Q-TOF instrument. A Shimadzu LC-20AT equipped with a SPD-M20A PDA detector was used for HPLC and a YMC-pack ODS-A column (250 × 10 mm, S-5 μm, 12 nm) were used for semipreparative HPLC separation. Silica gel (300–400 mesh, Qingdao Haiyang Chemical Co., Ltd.), C<sub>18</sub> reversed-phase silica gel (12 nm, S-50 μm, YMC Co., Ltd.), Sephadex LH-20 gel (Amersham Biosciences), and MCI gel (CHP20P, 75–150 μm, Mitsubishi Chemical Industries Ltd.) were used for column chromatography. All solvents used were of analytical grade (Guangzhou Chemical Reagents Company, Ltd.).

### 2.2. Plant material

The whole plant of *Chloranthus japonicus* Sieb. was collected in May 2013 from Yunnan Province, P. R. China, and was authenticated by Prof. You-Kai Xu of Xishuangbanna Tropical Botanical Garden, Chinese Academy of Sciences. A voucher specimen (accession number: SKW201305) has been deposited at the School of Pharmaceutical Sciences, Sun Yat-sen University.

### 2.3. Extraction and isolation

The air-dried powder of the whole plant of *C. japonicus* (1.0 kg) was extracted with 95% EtOH (3 × 3L) at room temperature to give 100 g of crude extract. The extract was suspended in H<sub>2</sub>O (1L) and successively partitioned with petroleum ether (PE, 3 × 1 L), EtOAc (3 × 1 L), and *n*-BuOH (3 × 1L). The EtOAc extract (60 g) was subjected to MCI gel column chromatography (CC) with a MeOH/H<sub>2</sub>O gradient (3:7 → 10:0) to afford five fractions (I–V). Fraction III (3 g) was chromatographed over a silica gel CC eluted with PE/acetone (80:1 → 2:1) to afford four fractions (IIIa–IIIId). Fraction IIIb (208 mg) was separated on C<sub>18</sub> reversed-phase (RP-18) silica gel CC

eluted with MeOH/H<sub>2</sub>O (5:5 → 10:0), followed by silica gel CC (CH<sub>2</sub>Cl<sub>2</sub>/MeOH, 200:1) and Sephadex LH-20 column (CH<sub>2</sub>Cl<sub>2</sub>/MeOH, 1:1) to afford **1** (15 mg). Further purification of fraction III d (1 g) by silica gel CC (PE/acetone, 40:1 → 5:1) and silica gel CC (CH<sub>2</sub>Cl<sub>2</sub>/MeOH, 200:1) to give **4** (500 mg). Fraction IV (2.5 g) was separated by RP-18 silica gel CC using a MeOH/H<sub>2</sub>O gradient (6:4 → 10:0) to give three fractions (IVa–IVc). Fraction IVb (1.7 g) was subjected successively to Sephadex LH-20 column (CH<sub>2</sub>Cl<sub>2</sub>/MeOH, 1:1) and a silica gel CC (PE/EtOAc, 80:1) to yield **2** (1.0 g) and **3** (300 mg).

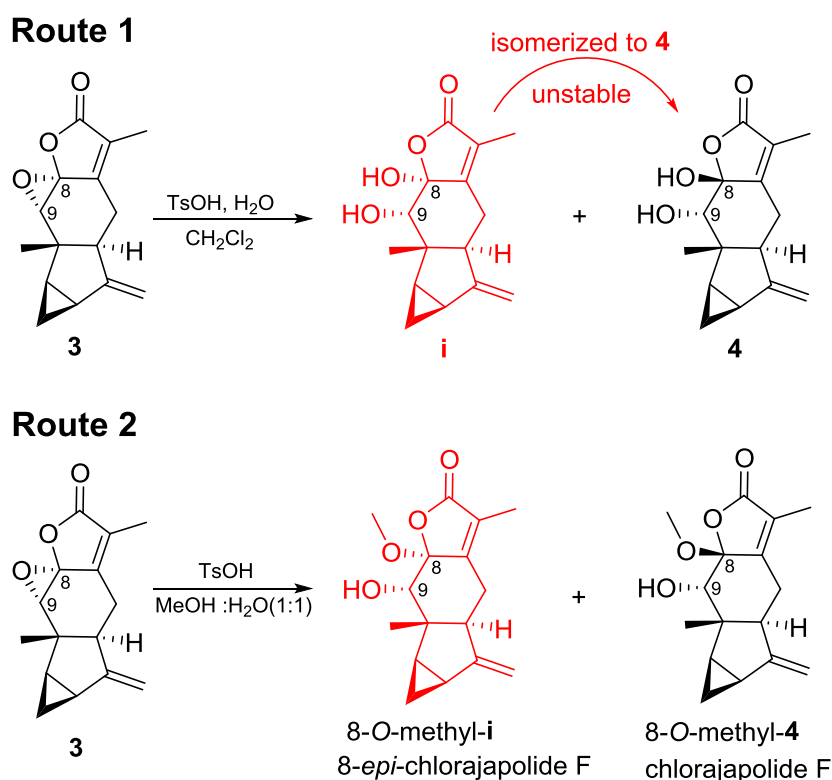
#### 2.4. Semisynthesis of chloranerectuslactone V (**5**) from **3**

A stirred solution of **3** (15.0 mg, 0.06 mmol) in CH<sub>2</sub>Cl<sub>2</sub> was treated with an aqueous solution of *p*-toluenesulfonic acid (1.9 mg, 0.1 ml, 0.01 mmol). The reaction mixture was stirred at room temperature for 2 h. The mixture was filtered through a short pad of silica gel washed with CH<sub>2</sub>Cl<sub>2</sub>. Evaporation of the solvent afforded the compound **4** (15.7 mg, 0.06 mmol) in 99% crude yield. Data for **4**: <sup>1</sup>H-NMR (400 MHz, CDCl<sub>3</sub>) δ<sub>H</sub> 6.02 (s, 1H), 4.99 (s, 1H), 4.70 (s, 1H), 3.94 (s, 1H), 3.38 (m, 1H), 2.52 (m, 1H), 2.21 (m, 1H), 1.98 (m, 2H), 1.79 (s, 3H), 0.80 (m, 1H), 0.66 (m, 1H), 0.52 (s, 3H) ppm; <sup>13</sup>C-NMR (100 MHz, CDCl<sub>3</sub>) δ<sub>C</sub> 173.8, 159.5, 151.9, 124.7, 106.2, 104.6, 77.2, 51.4, 43.3, 23.7, 22.9, 22.2, 19.9, 15.6, 8.2 ppm. Above data were identical to those of natural product chloranthalactone E.<sup>1,2</sup>

To a vigorously stirred suspension of chromatographic grade silica gel (225.0 mg, 3.7 mmol) in CH<sub>2</sub>Cl<sub>2</sub> (1 ml) was added dropwise an aqueous solution of NaIO<sub>4</sub> (22.50 mg, 0.1 ml, 0.11 mmol) whence a flaky suspension was formed. Then a solution of **4** (15.7 mg, 0.06 mmol) in CH<sub>2</sub>Cl<sub>2</sub> (0.2 ml) was added, and the resulting mixture was stirred at room temperature for 12 h. The mixture was filtered through a short pad of silica gel washed with CH<sub>2</sub>Cl<sub>2</sub>. Evaporation of the solvent under vacuum afforded the compound **ii** (13.1 mg, 0.05 mmol) in 83% crude yield, which was pure enough for use in the next step. Data for intermediate **ii**: <sup>1</sup>H-NMR (400 MHz, CDCl<sub>3</sub>) δ<sub>H</sub> 9.50 (s, 1H), 4.98 (s, 1H), 4.44 (s, 1H), 2.91 (dd, *J* = 12.0, 5.4 Hz, 1H), 2.54 (dd, *J* = 13.4, 5.4 Hz, 1H), 2.32 (m, 1H), 2.03 (s, 3H), 1.98 (m, 1H), 1.81 (m, 1H), 1.23 (s, 3H), 0.93 (m, 1H), 0.81 (m, 1H) ppm; <sup>13</sup>C-NMR (100 MHz, CDCl<sub>3</sub>) δ<sub>C</sub> 202.1, 165.8, 165.6, 152.0, 142.8, 142.2, 108.8, 55.9, 42.5, 27.8, 27.3, 24.7, 14.9, 11.3, 10.1 ppm. ESIMS *m/z* 259.1 [M – H]<sup>–</sup>.

Compound **ii** (13.1 mg, 0.05 mmol) was dissolved in MeOH/H<sub>2</sub>O (1:1, 1 ml), and aqueous solution of *p*-toluenesulfonic acid (1.9 mg, 0.1 ml, 0.01 mmol) was added dropwise. The mixture was stirred at 50 °C for 28 h and the resulting product was purified by flash chromatography on silica gel to give **5** (12.6 mg, 0.04 mmol) in 80% crude yield. Data for **5**: <sup>1</sup>H-NMR (400 MHz, CDCl<sub>3</sub>) δ<sub>H</sub> 9.60 (s, 1H), 3.77 (s, 3H), 2.59 (m, 1H), 2.48 (m, 1H), 2.00 (m, 1H), 1.99 (s, 3H), 1.76 (m, 1H), 1.66 (m, 1H), 1.53 (s, 3H), 1.21 (s, 3H), 0.81 (m, 1H), 0.73 (m, 1H) ppm; <sup>13</sup>C-NMR (100 MHz, CDCl<sub>3</sub>) δ<sub>C</sub> 202.1, 170.2, 166.3, 139.2, 127.0, 91.6, 56.8, 52.7, 44.4, 31.4, 28.9, 27.0, 25.5, 16.5, 15.6, 7.4 ppm. Above data were identical to those of natural product chloranerectuslactone V.<sup>3</sup>

2.5. Demonstration of the existence of compound **i** in acid-catalyzed epoxy ring-opening reaction system of **3**



**Scheme 1** Acid-catalyzed epoxy ring-opening of **3**.

In the above acid-catalyzed epoxy ring-opening systems (Scheme 1, Route 1), two products (**i** and **4**) were supposed to be generated. However, we could only detect the expected products by TLC but fail to get the pure **i** due to its tautomerization to **4**. So the reaction was modified by adding the MeOH in the system (Scheme 1, Route 2), which successfully captured the unstable **i** by forming its 8-*O*-methyl derivative.

Compound **3** (7.5 mg, 0.03 mmol) was dissolved in MeOH/H<sub>2</sub>O (1:1, 1 ml), and aqueous solution of *p*-toluenesulfonic acid (1.9 mg, 0.1 ml, 0.01 mmol) was added dropwise. The reaction mixture was stirred at room temperature for 2 h. The mixture was purified by silica gel column chromatography (PE/EtOAc, 50:1 → 20:1) to afford **8-O-methyl-i** (3.0 mg, 0.011 mmol) and **8-O-methyl-4** (3.3 mg, 0.012 mmol). Data for **8-O-methyl-i**: <sup>1</sup>H-NMR (400 MHz, CDCl<sub>3</sub>) δ<sub>H</sub> 5.01 (d, *J* = 2.4 Hz, 1H), 4.70 (s, 1H), 3.84 (s, 1H), 3.32 (m, 1H), 3.22 (s, 3H), 2.30 (m, 2H), 2.11 (m, 1H), 1.97 (m, 1H), 1.88 (s, 3H), 0.83 (m, 1H), 0.68 (m, 1H), 0.50 (s, 3H) ppm; Data for **8-O-methyl-4**: <sup>1</sup>H-NMR (400 MHz, CDCl<sub>3</sub>) δ<sub>H</sub> 5.00 (d, *J* = 0.8 Hz, 1H), 4.73 (s, 1H), 4.08 (d, *J* = 1.6 Hz, 1H), 3.18 (s, 3H), 2.97 (dd, *J* = 13.0, 2.5 Hz, 1H), 2.55 (dd, *J* = 13.0, 2.5 Hz, 1H), 2.35 (d, *J* = 2.0 Hz, 1H), 1.97 (dd, *J* = 13.0, 13.0 Hz, 1H), 1.89 (s, 3H), 0.93 (m, 1H), 0.89 (s, 3H), 0.79 (m, 1H) ppm.

**8-O-methyl-i** and **8-O-methyl-4** were previously reported as natural products 8-*epi*-chlorajapolide F and chlorajapolide F, respectively.<sup>4</sup> The NMR data of synthetic compounds were consistent with those reported in literature. (<sup>1</sup>H NMR Spectra please see S31†)

1. Takeda, Y.; Yamashita, H.; Matsumoto, T.; Terao, H. *Phytochemistry* **1993**, *33*, 713-715.

2. Li, X.; Zhang, Y. F.; Yang, L.; Feng, Y.; Liu, Y. M.; Zeng, X. *Acta pharmaceutica Sinica* **2011**, *46*, 1349-1351.

3. Huong, T. T.; Van, T. N.; Minh, T. T.; Tram, L. H.; Anh, N. T.; Cuong, H. D.; Van, C. P.; Ca, D. V. *Lett. Org. Chem.* **2014**, *11*, 639-642.

4. Zhang, M.; Wang, J. S.; Wang, P. R.; Oyama, M.; Luo, J.; Ito, T.; Iinuma, M.; Kong, L. Y. *Fitoterapia* **2012**, *83*, 1604-1609.

## 2.6. Nitric oxide (NO) production assays

The macrophages were supplemented with 3.0 mM glutamine, antibiotics (100 U/ml penicillin and 100 U/ml streptomycin), and 10% heat-inactivated fetal bovine serum at 37 °C under a humidified atmosphere of 5% CO<sub>2</sub>. The NO concentration was detected by the Griess reagent. RAW 264.7 cells were cultured onto 96-well plates at a density of 1 × 10<sup>5</sup> cells/well and stimulated with 1.0 μg/ml LPS (*Escherichia coli* 0111: B4, Sigma, St. Louis, MO, USA) in the presence or absence of test compounds. After incubation at 37 °C for 24 h, each 50 μl of culture supernatant was mixed with an equal volume of Griess reagent (0.1% N-1-naphthylethylenediamine

dihydrochloride, 1.0% sulfanilamide in 2.5% phosphoric acid solution) and incubated at room temperature for 10 min. The absorbance at 540 nm was measured in a microplate reader (Molecular Devices, USA) and compared with a calibration curve prepared using NaNO<sub>2</sub> standards. The experiments were performed in triplicate, and the data are expressed as the means ± SD of three independent experiments. Cell viability was determined initially by the MTT method to determine if the inhibition of NO production was due to the cytotoxicity. As a result, no obvious cytotoxic effect (over 90% cell survival) was observed at concentrations up to 100 μM on RAW 264.7 cells. Quercetin was used as a positive control. All the compounds were prepared as stock solutions in DMSO (final solvent concentration less than 0.5% in all assays).

**Table 2.** Inhibition against LPS-activated NO production in RAW 264.7 macrophages of compounds **1–5**.

Compound	IC <sub>50</sub> (μM) <sup>a</sup>	Compound	IC <sub>50</sub> (μM) <sup>a</sup>
<b>1</b>	14.87 ± 0.98	<b>4</b>	> 30
<b>2</b>	> 30	<b>5</b>	> 30
<b>3</b>	29.19 ± 0.65	quercetin <sup>b</sup>	15.90 ± 0.68

<sup>a</sup> Values are represented as means ± SD based on three independent experiments, <sup>b</sup> Positive control.

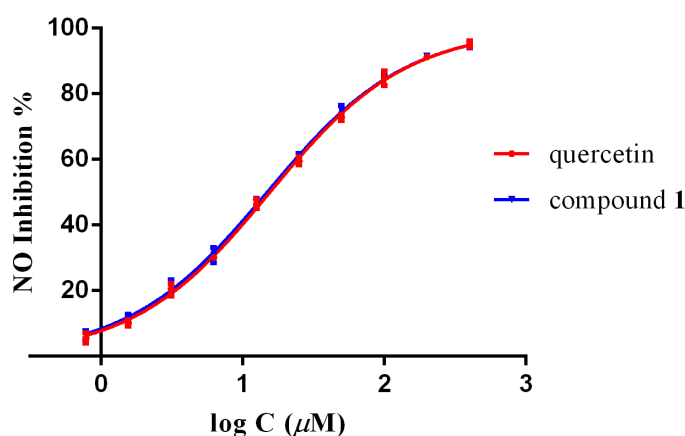
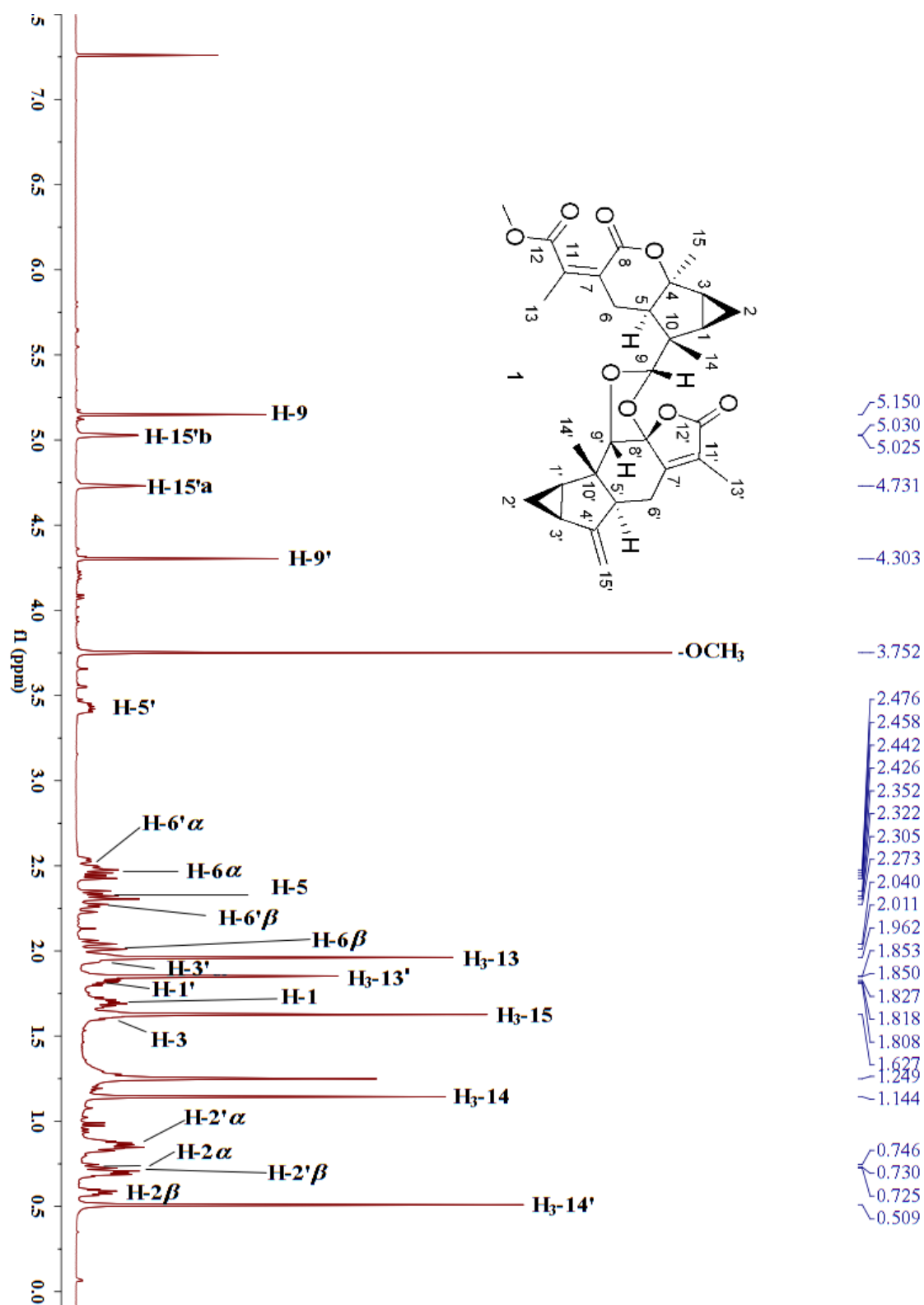


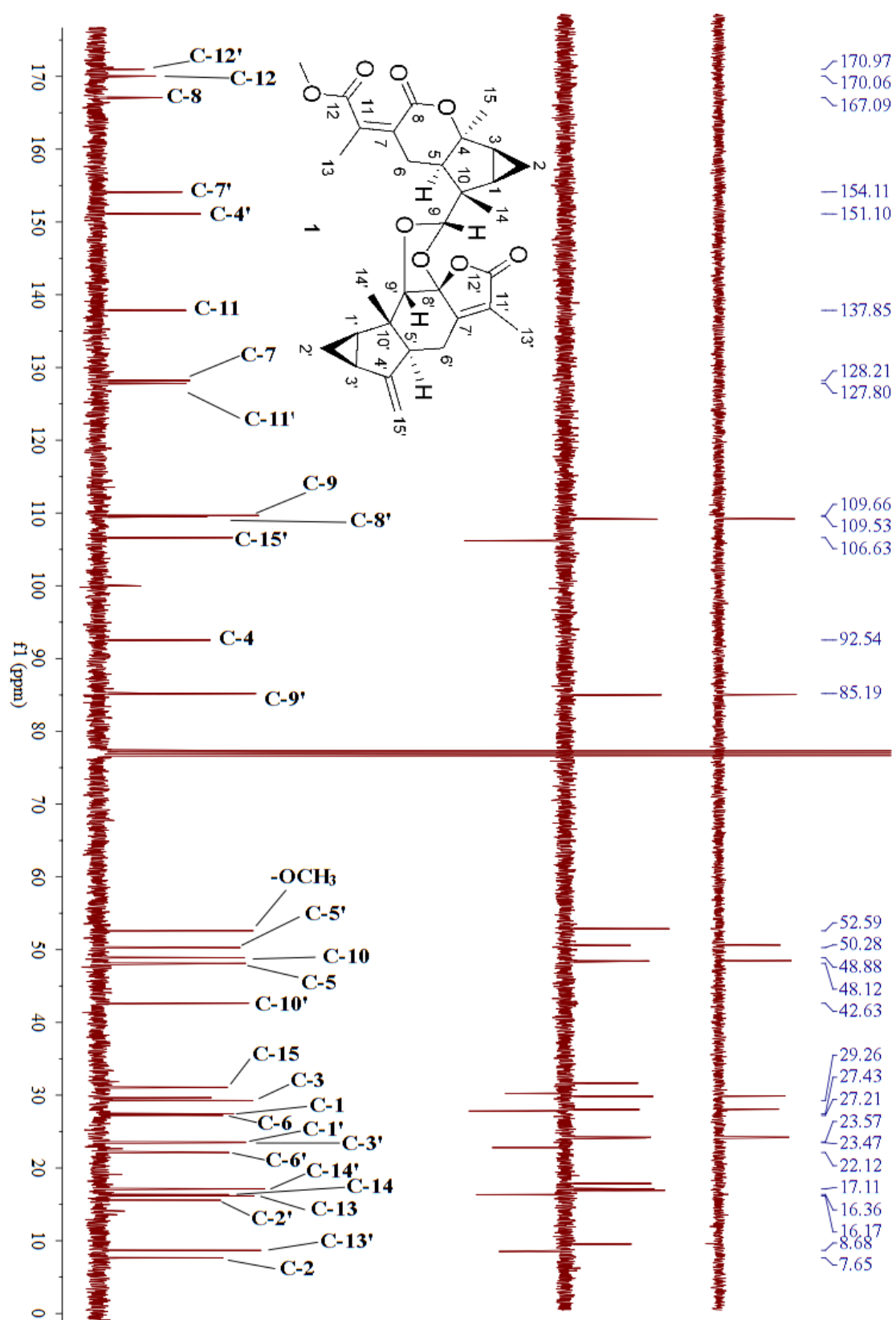
**Figure 1.** The inhibition curves of compound **1** against LPS-activated NO production in RAW 264.7 macrophages



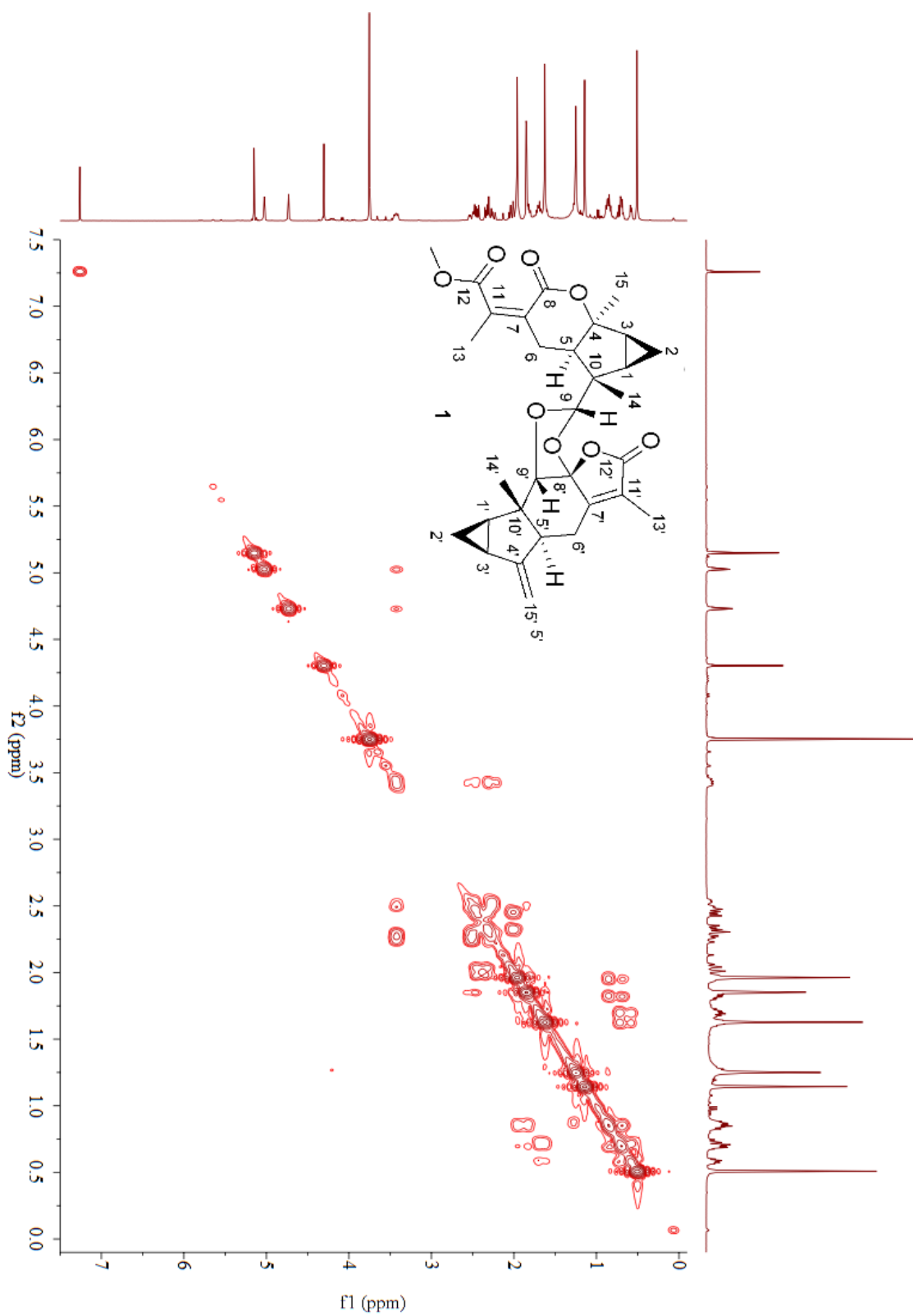
S3.  $^1\text{H}$  NMR (400 MHz,  $\text{CDCl}_3$ ) spectrum of chlojapolactone A (**1**)



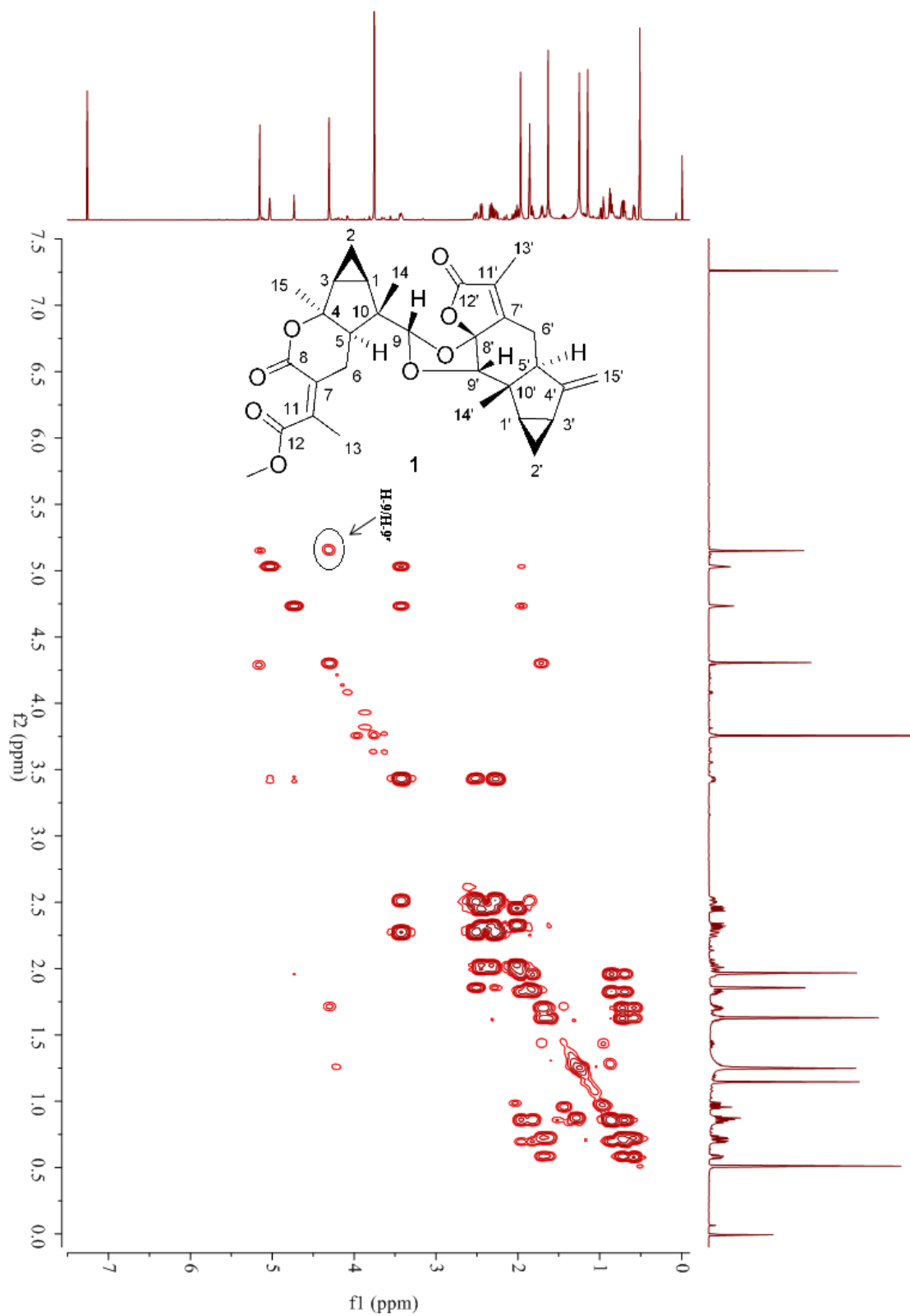
S4.  $^{13}\text{C}$  NMR (100 MHz,  $\text{CDCl}_3$ ) spectrum of chlojapolactone A (**1**)



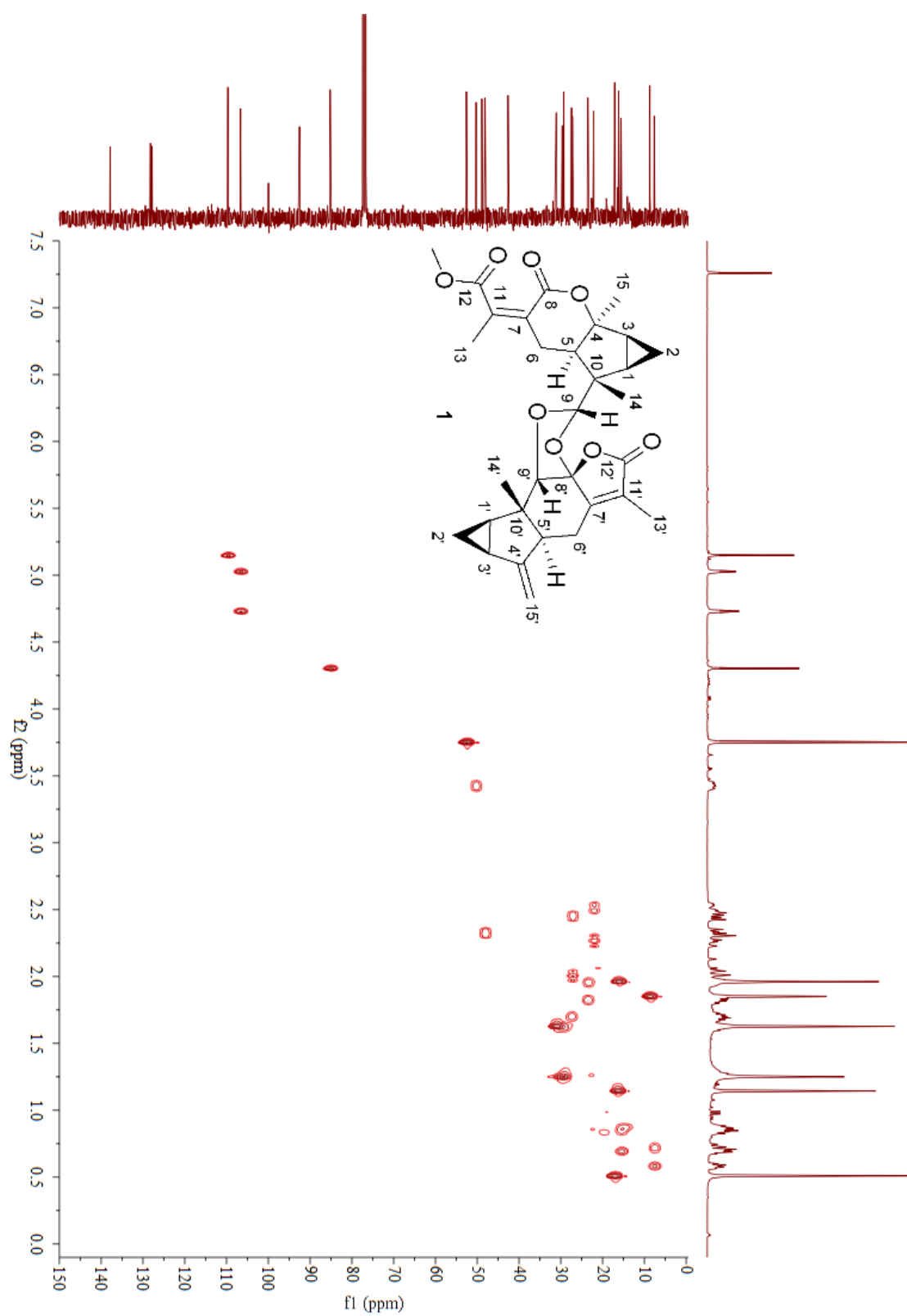
S5.  $^1\text{H}$ - $^1\text{H}$  COSY spectrum of chlojapolactone A (**1**) in  $\text{CDCl}_3$



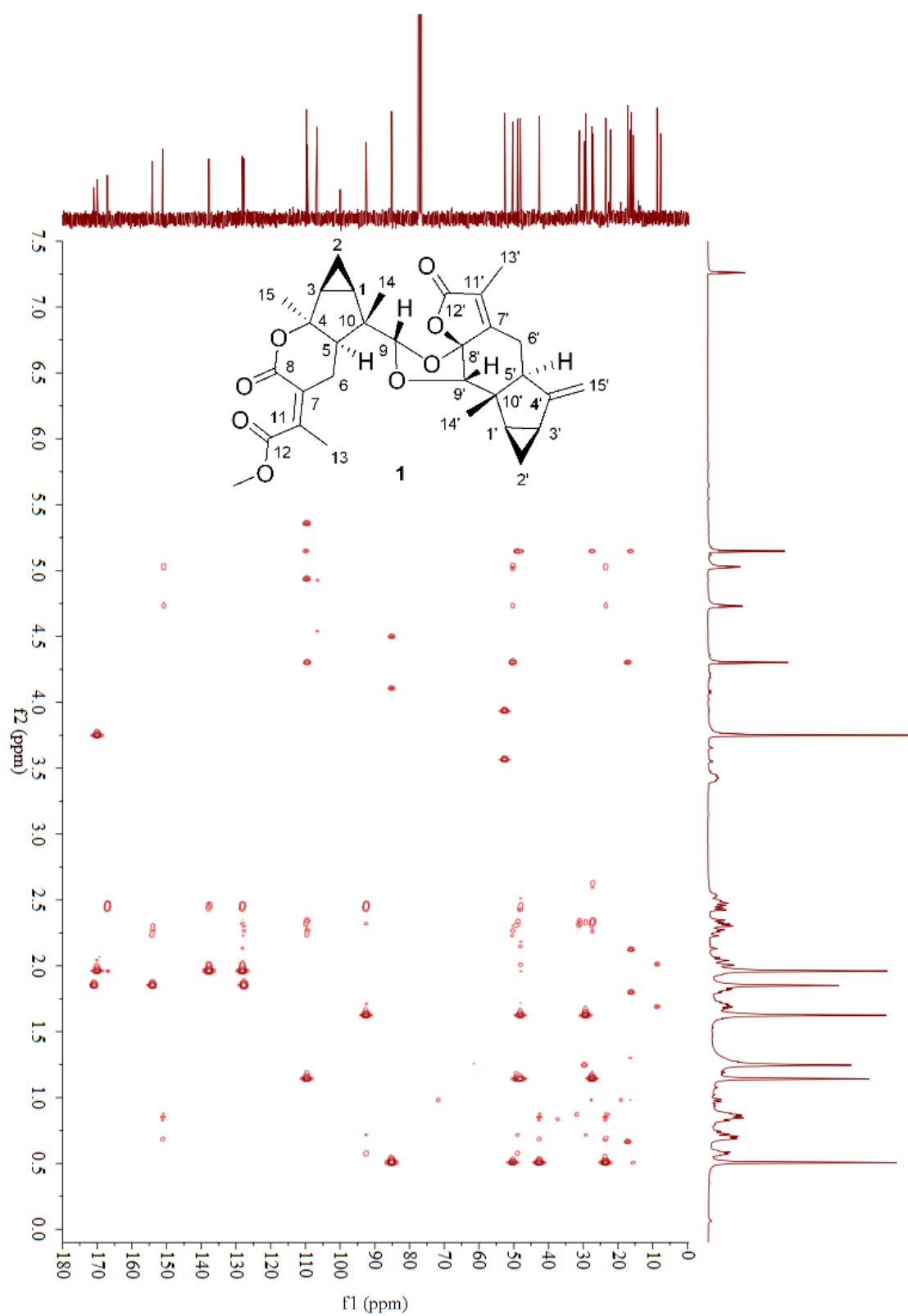
S6. Long rang  $^1\text{H}$ - $^1\text{H}$  COSY spectrum of chlojapolactone A (**1**) in  $\text{CDCl}_3$



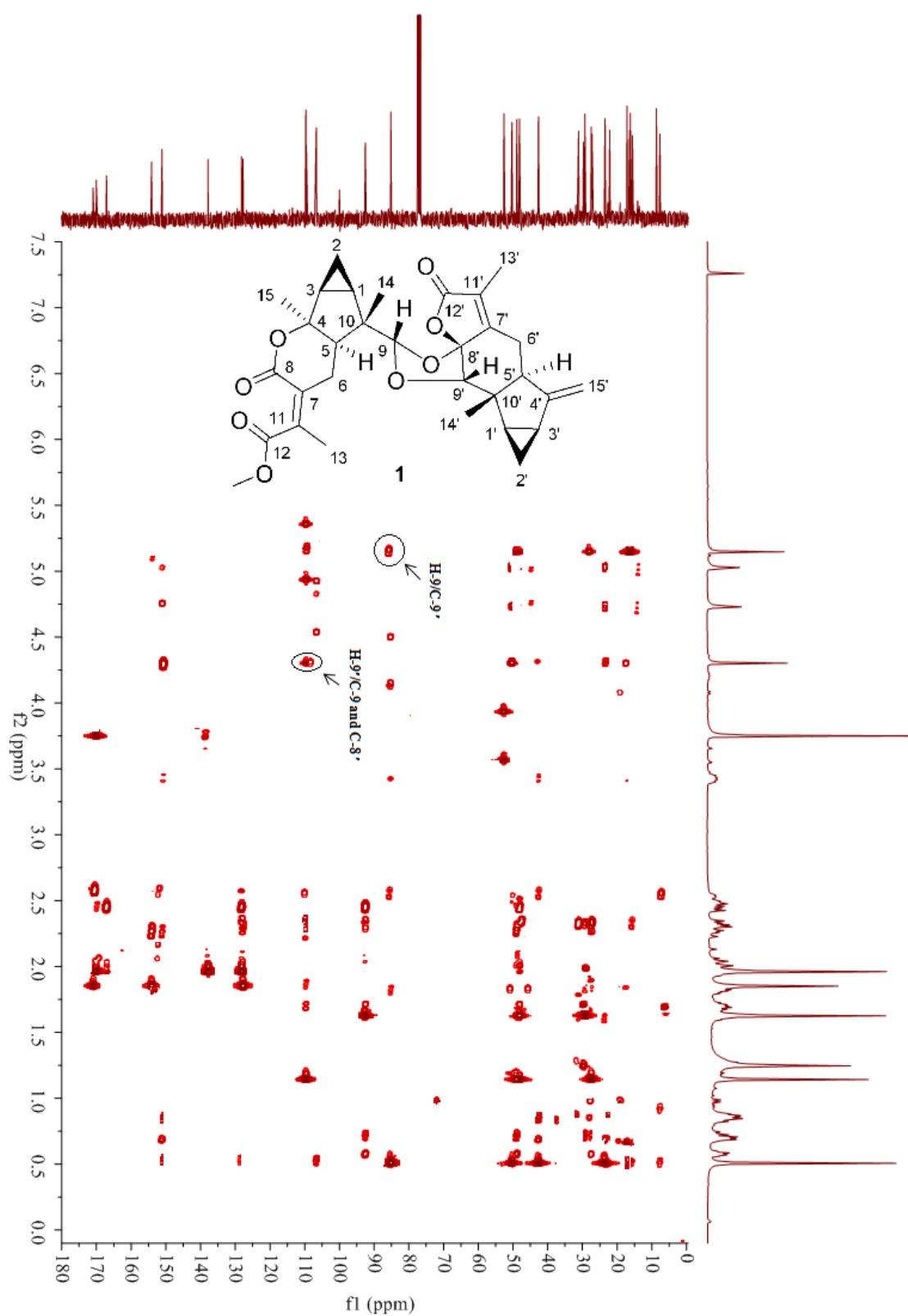
S7. HSQC spectrum of chlojapolactone A (**1**) in CDCl<sub>3</sub>



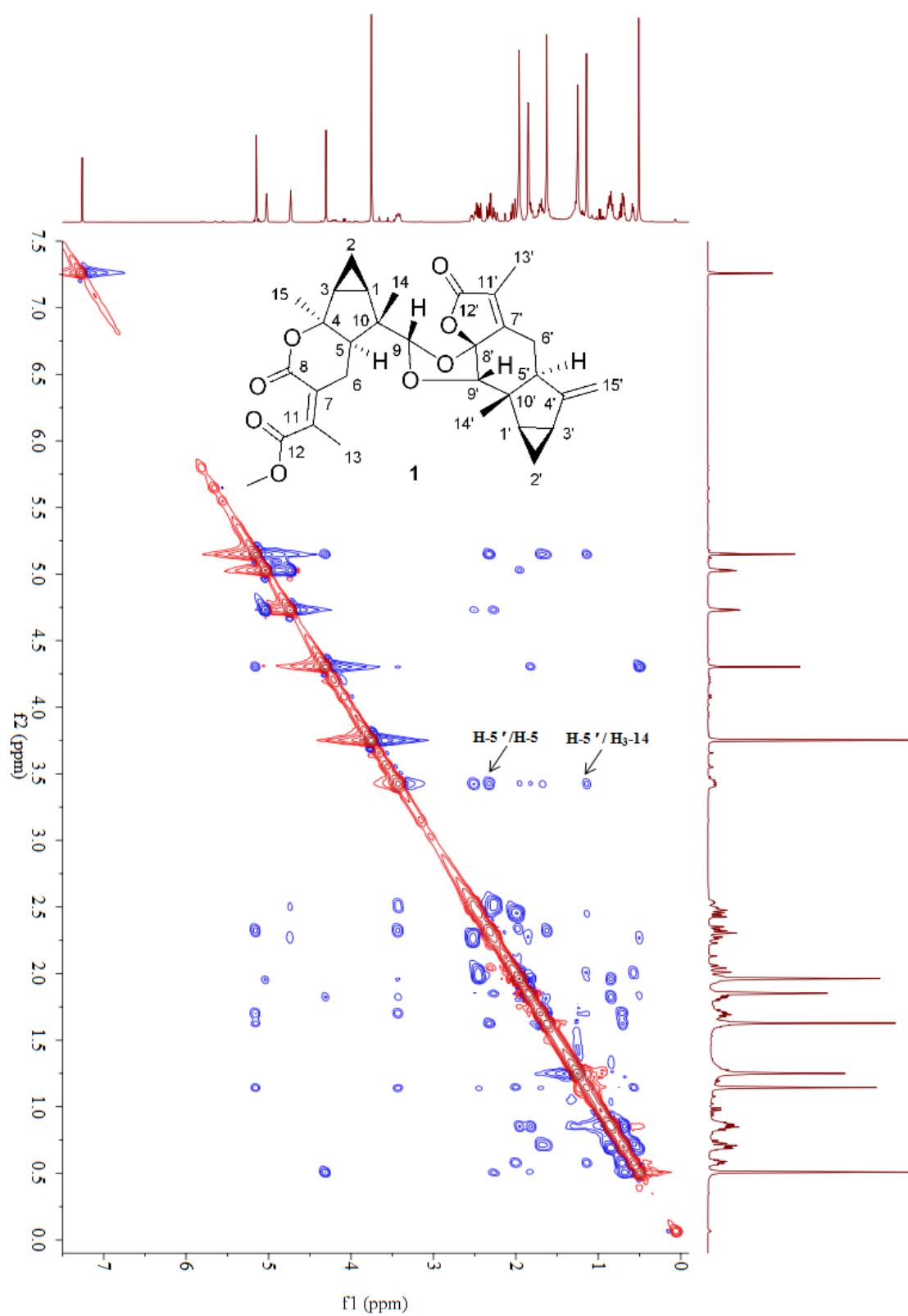
S8. HMBC spectrum of chlojapolactone A (**1**) in CDCl<sub>3</sub>



S9. Modified HMBC spectrum of chlojapolactone A (**1**) in CDCl<sub>3</sub>

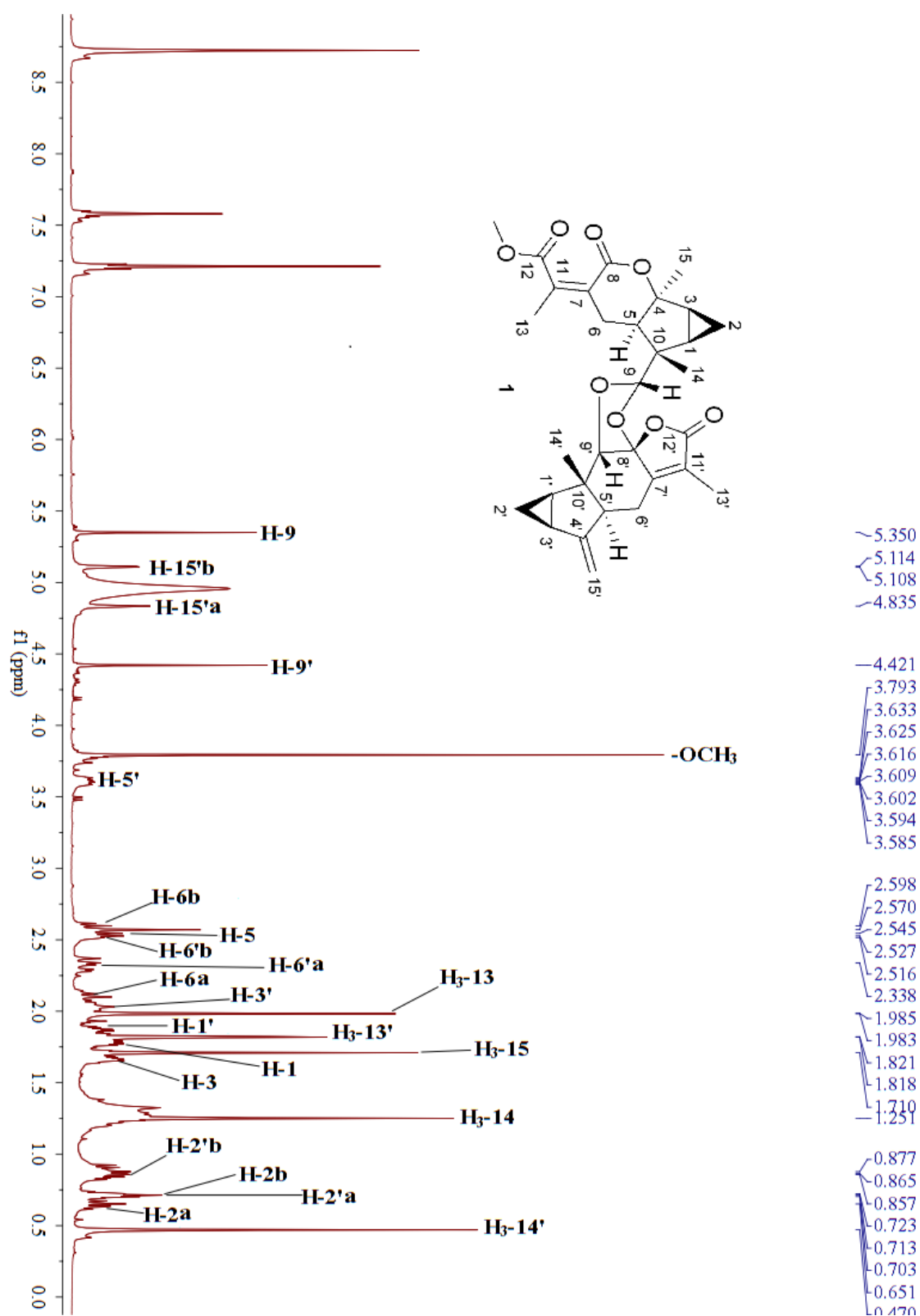


S10. ROESY spectrum of chlojapolactone A (**1**) in CDCl<sub>3</sub>

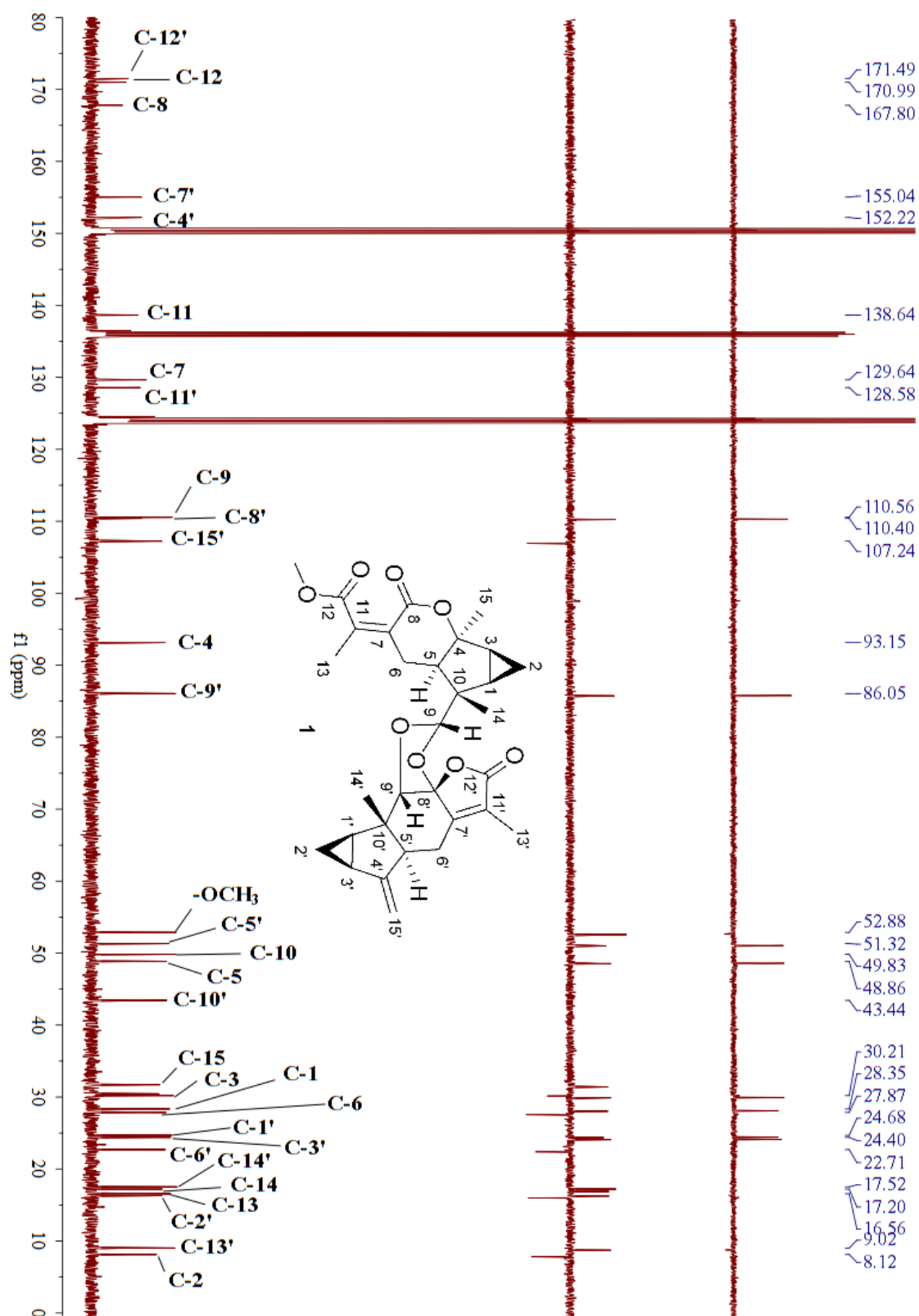




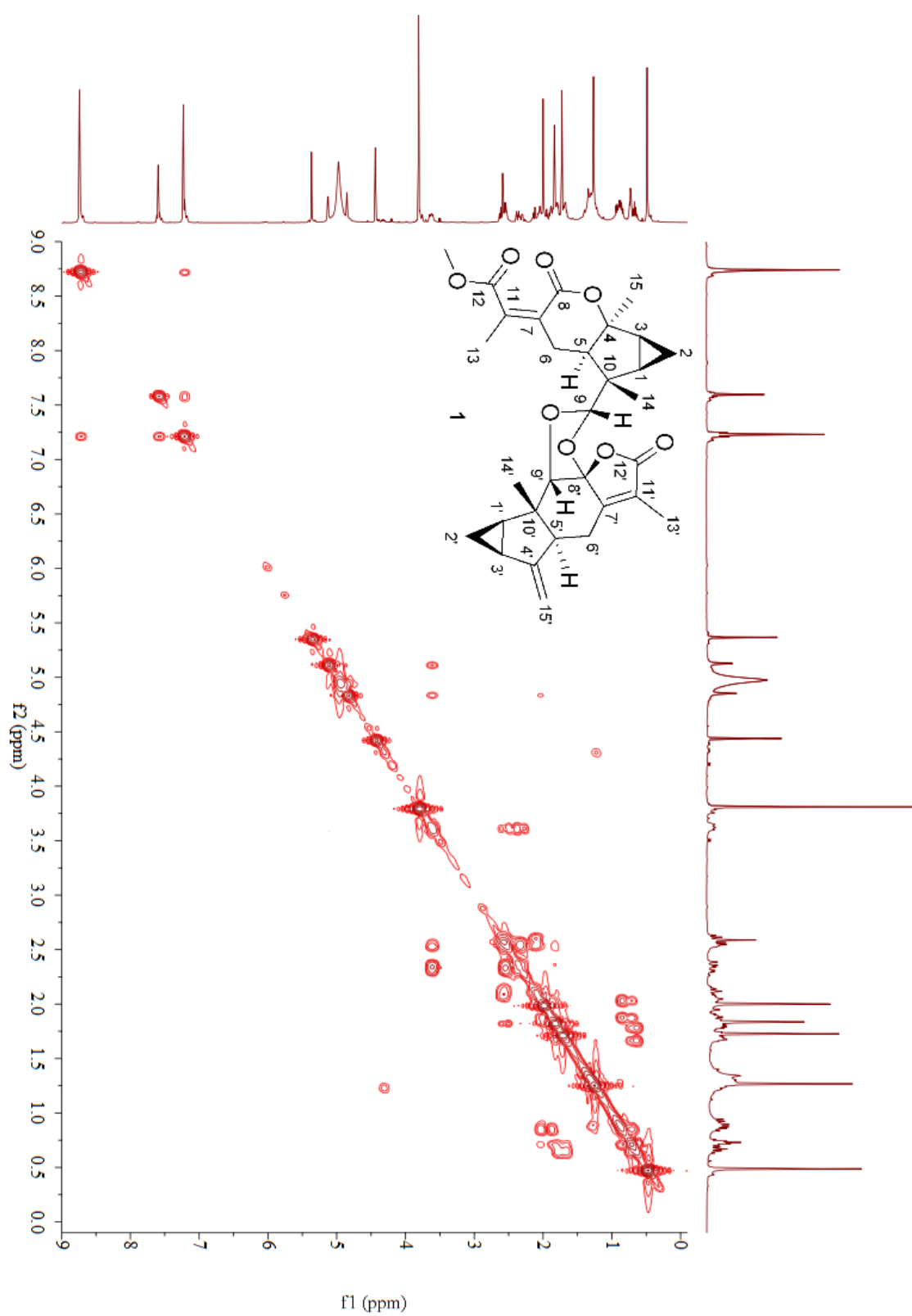
S11.  $^1\text{H}$  NMR (500 MHz,  $\text{C}_5\text{D}_5\text{N}$ ) spectrum of chlojapolactone A (**1**)



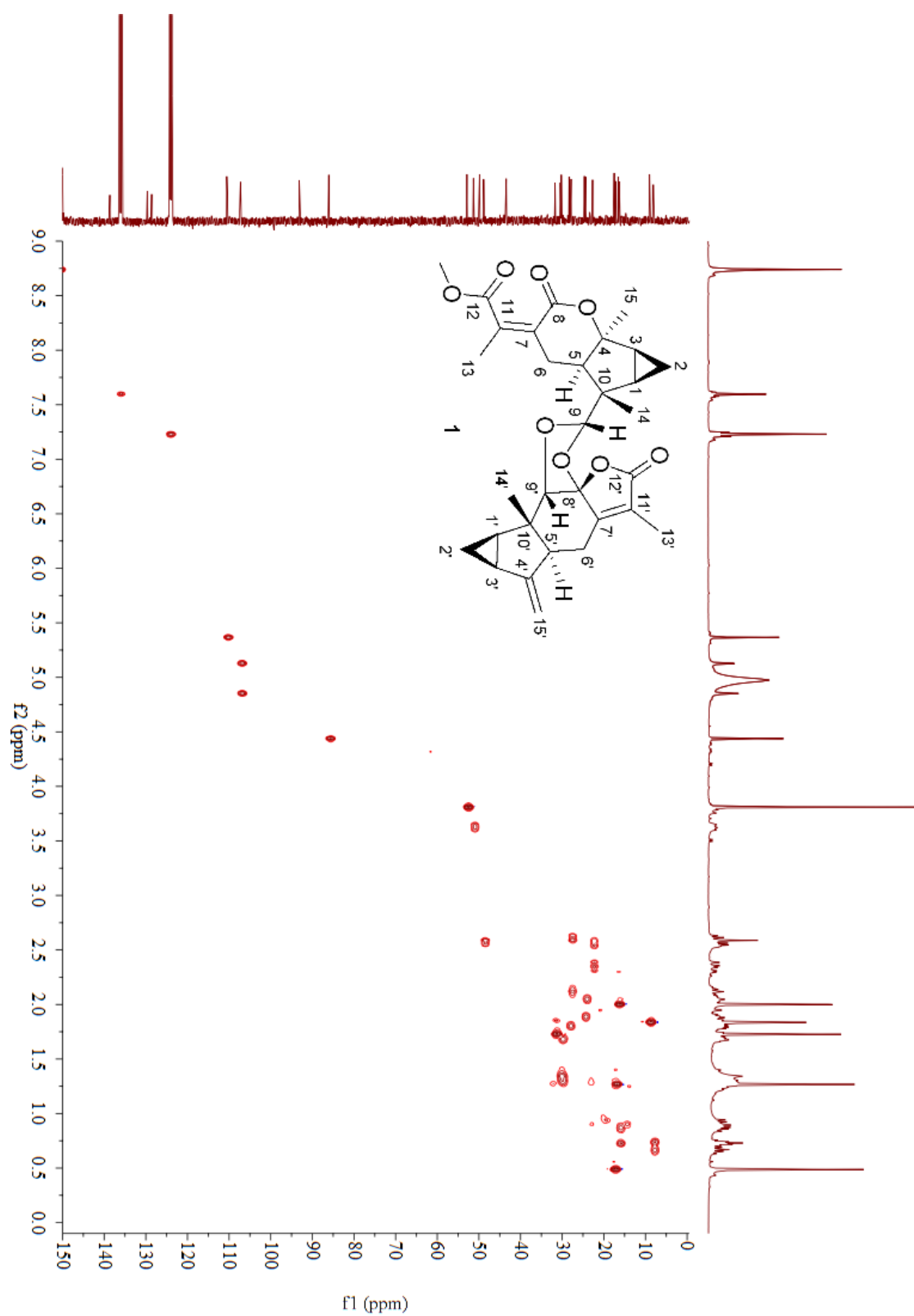
S12.  $^{13}\text{C}$  NMR (125 MHz,  $\text{C}_5\text{D}_5\text{N}$ ) spectrum of chlojapolactone A (**1**)



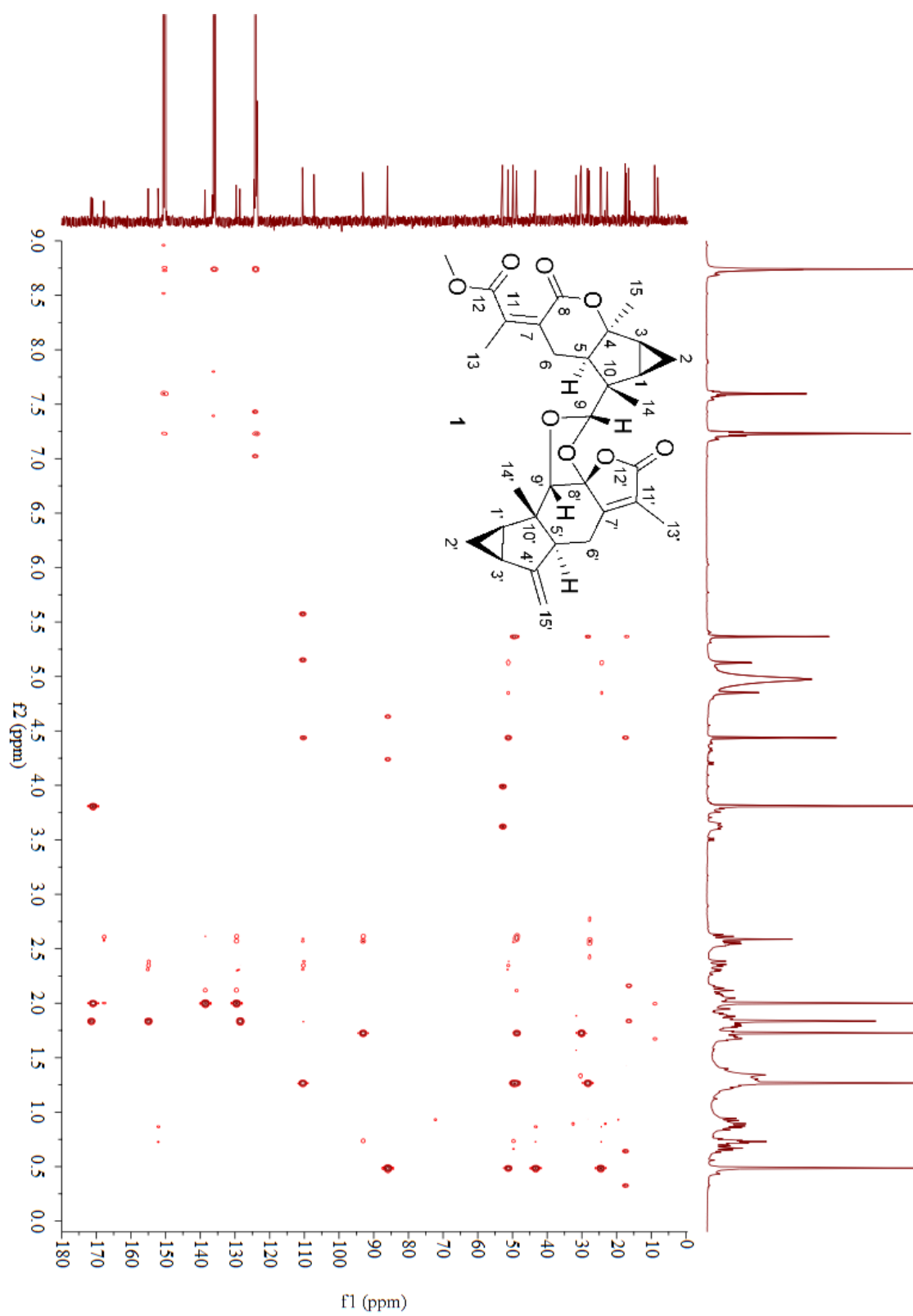
S13.  $^1\text{H}$ - $^1\text{H}$  COSY spectrum of chlojapolactone A (**1**) in  $\text{C}_5\text{D}_5\text{N}$



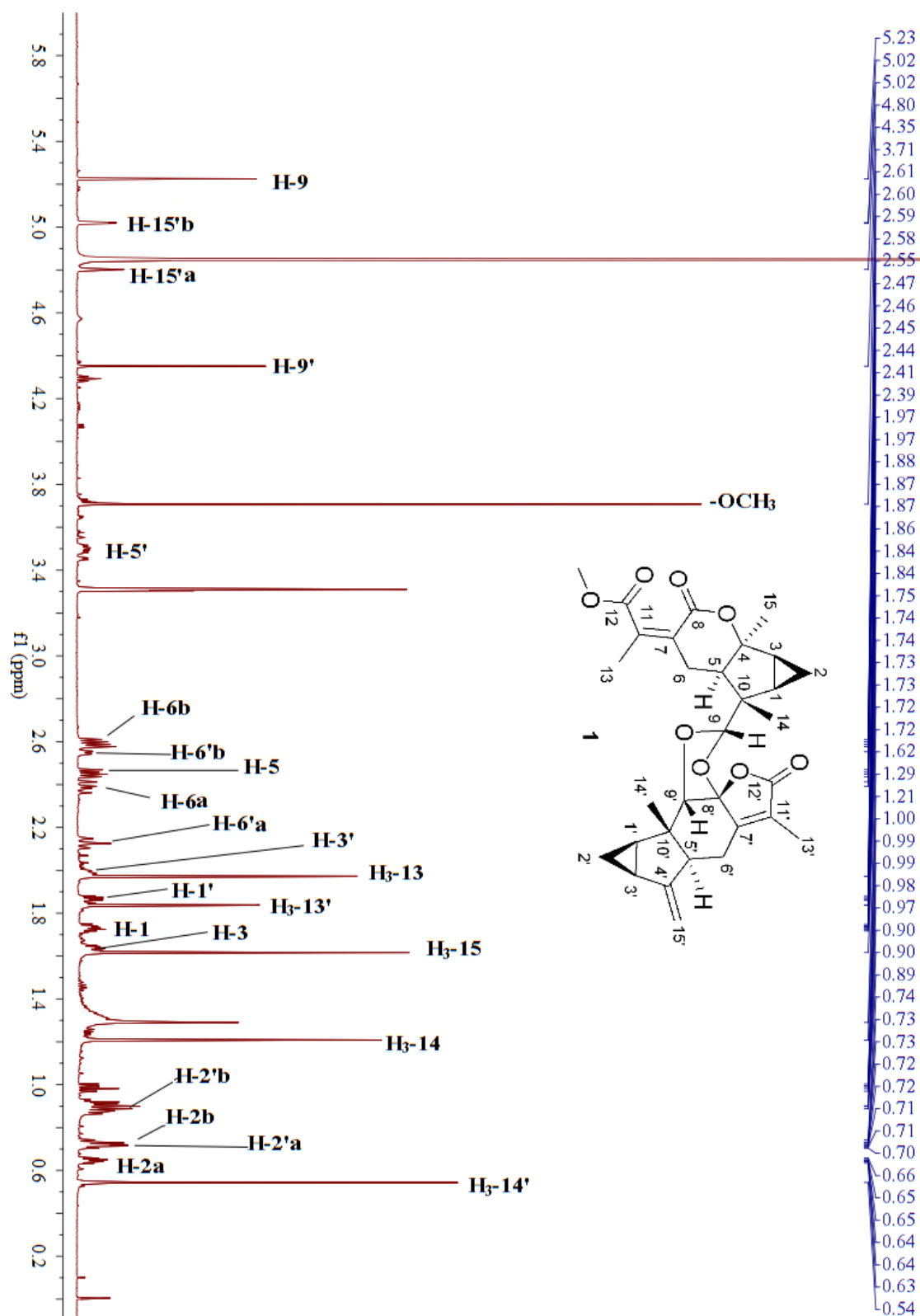
S14. HSQC spectrum of chlojapolactone A (**1**) in C<sub>5</sub>D<sub>5</sub>N



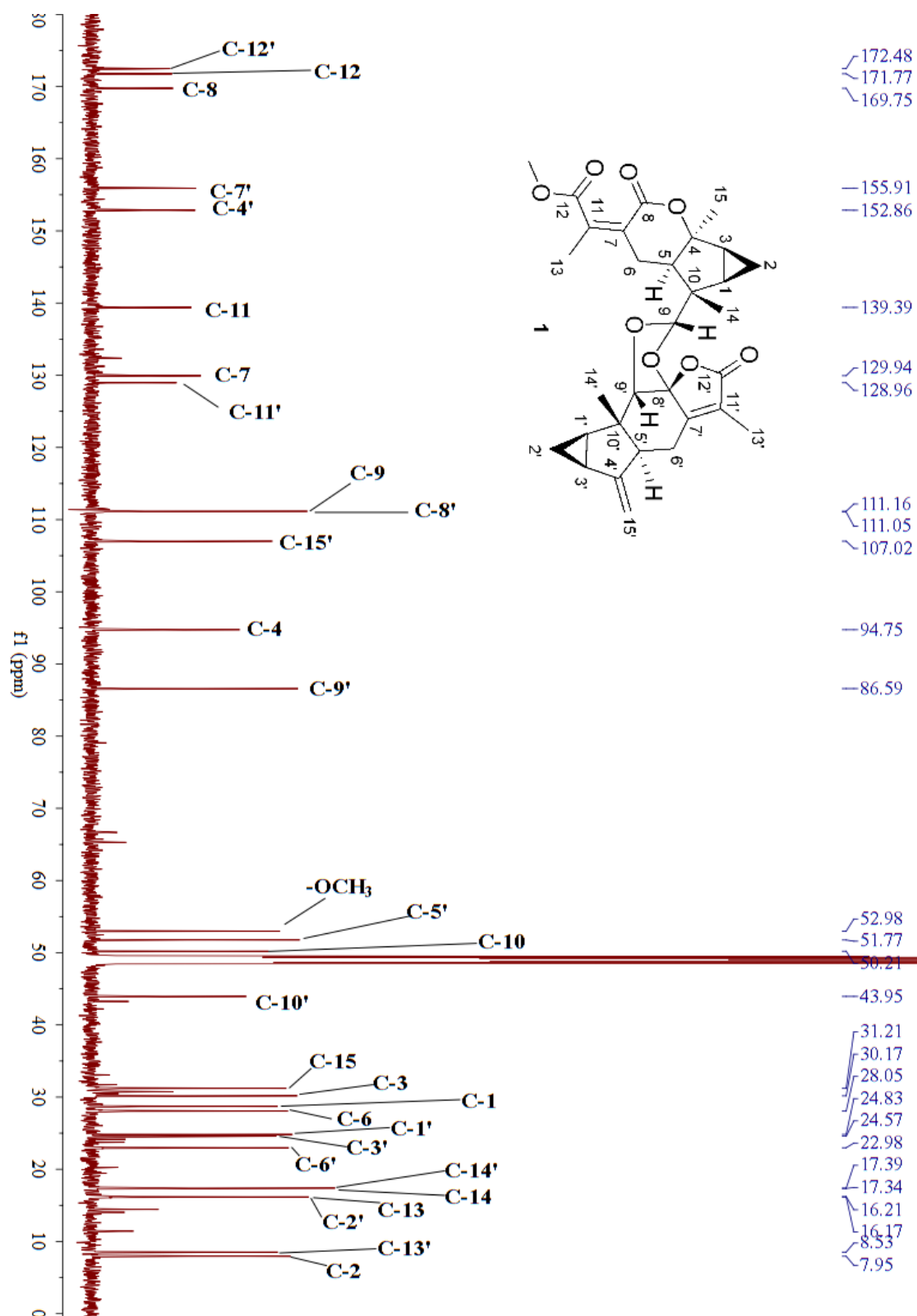
S15. HMBC spectrum of chlojapolactone A (**1**) in C<sub>5</sub>D<sub>5</sub>N



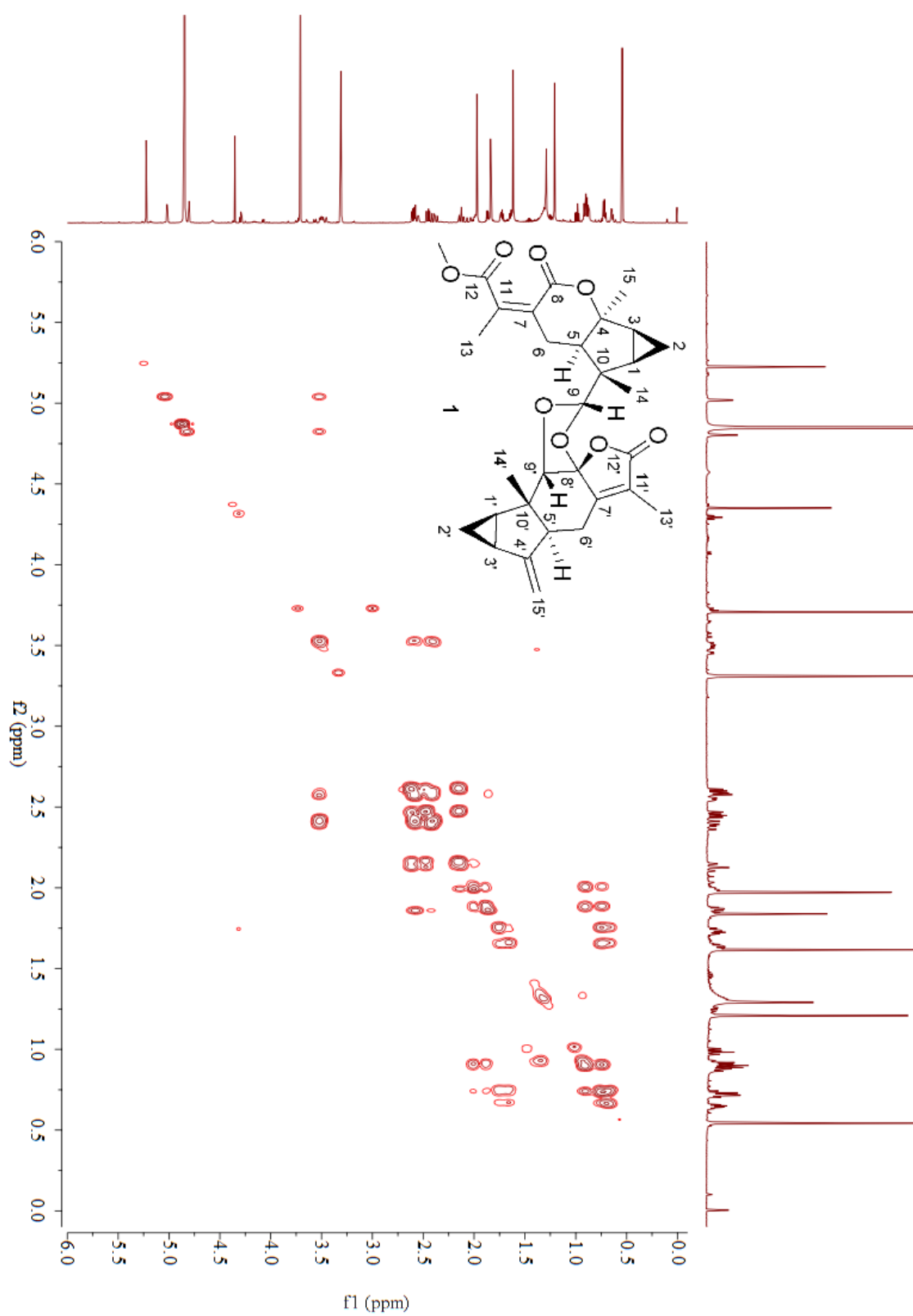
S16.  $^1\text{H}$  NMR (600 MHz,  $\text{CD}_3\text{OD}$ ) spectrum of chlojapolactone A (**1**)



S17.  $^{13}\text{C}$  NMR (150 MHz,  $\text{CD}_3\text{OD}$ ) spectrum of chlojapolactone A (**1**)

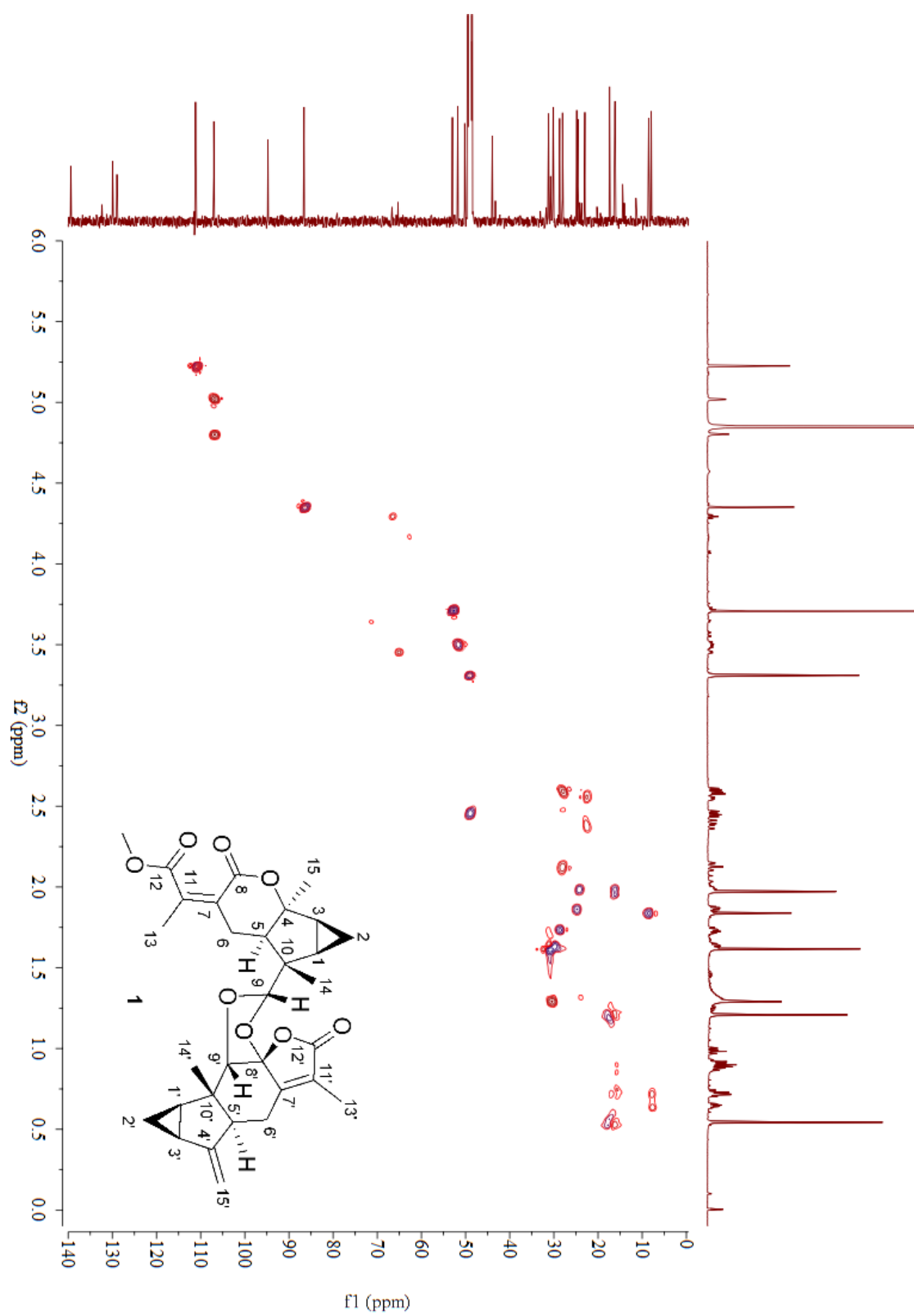


S18.  $^1\text{H}$ - $^1\text{H}$  COSY spectrum of chlojapolactone A (**1**) in  $\text{CD}_3\text{OD}$

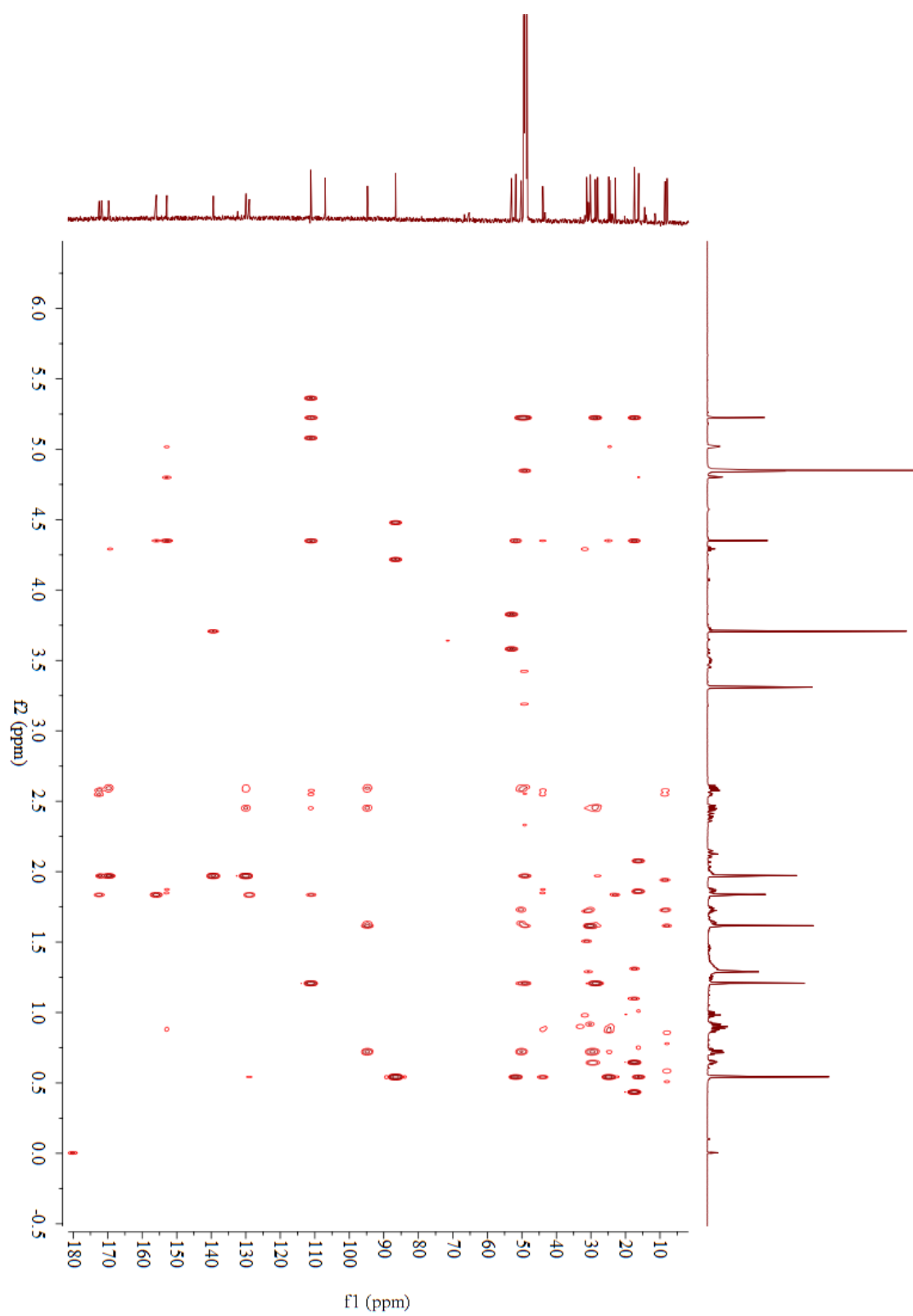




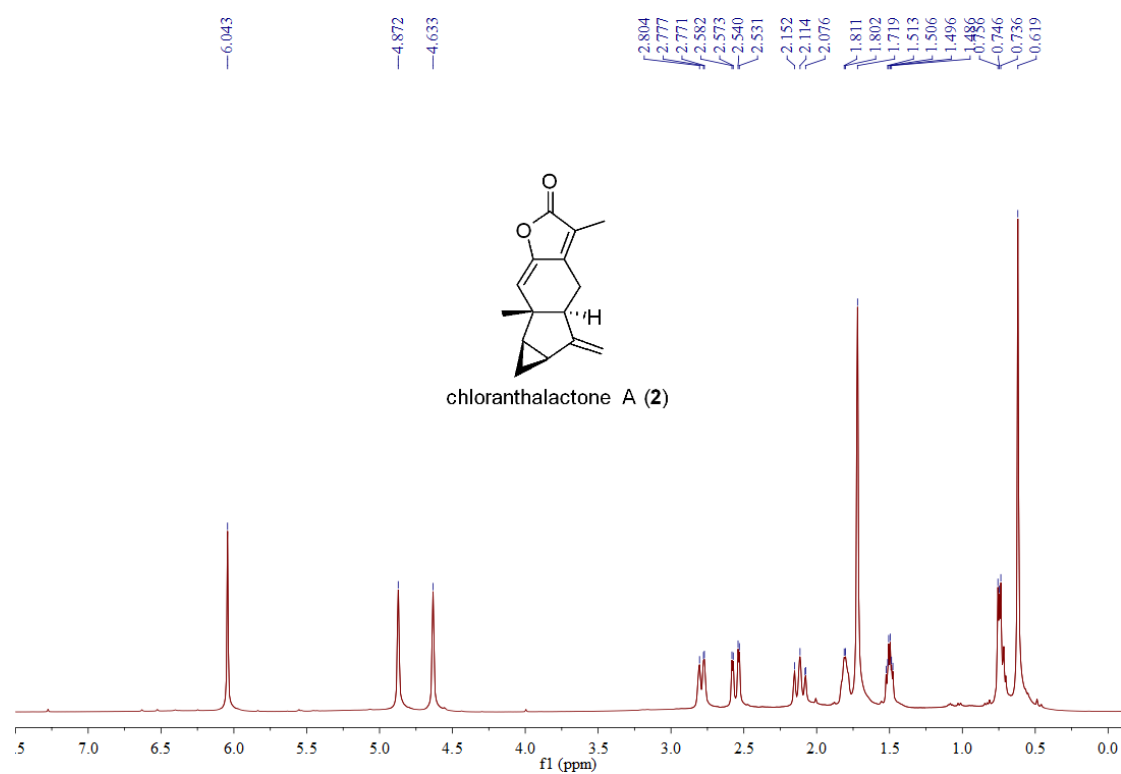
S19. HSQC spectrum of chlojapolactone A (**1**) in CD<sub>3</sub>OD



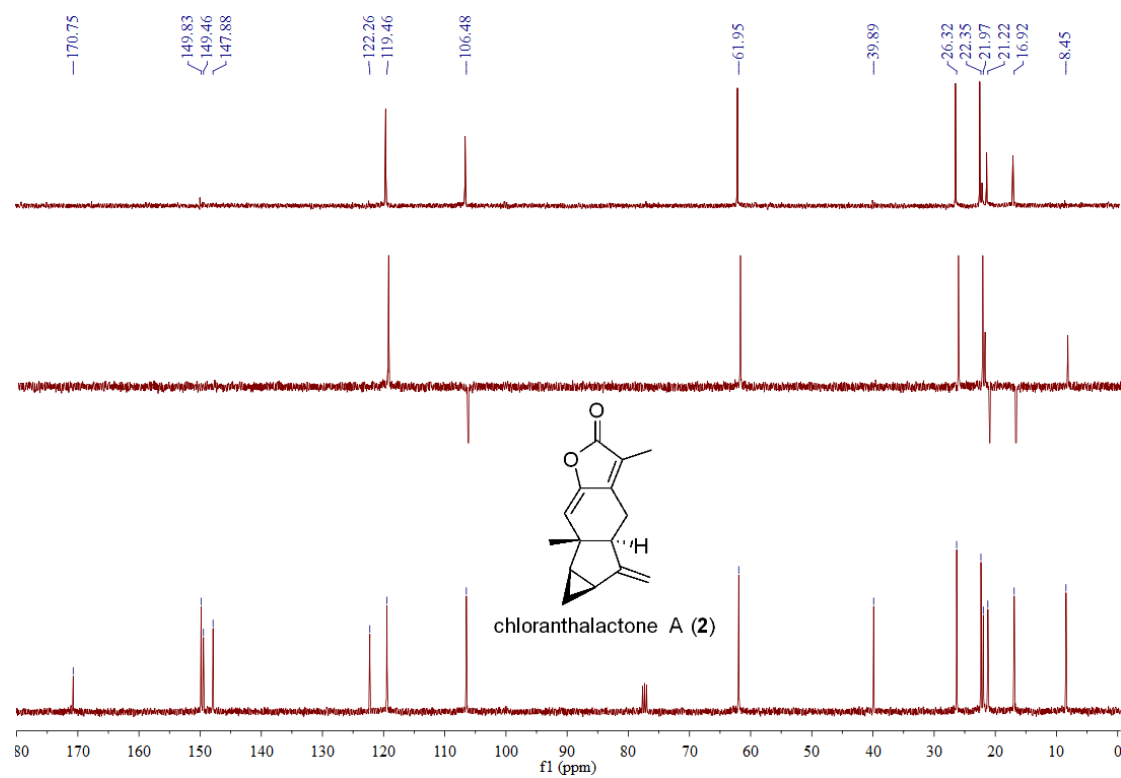
S20. HMBC spectrum of chlojapolactone A (**1**) in CD<sub>3</sub>OD



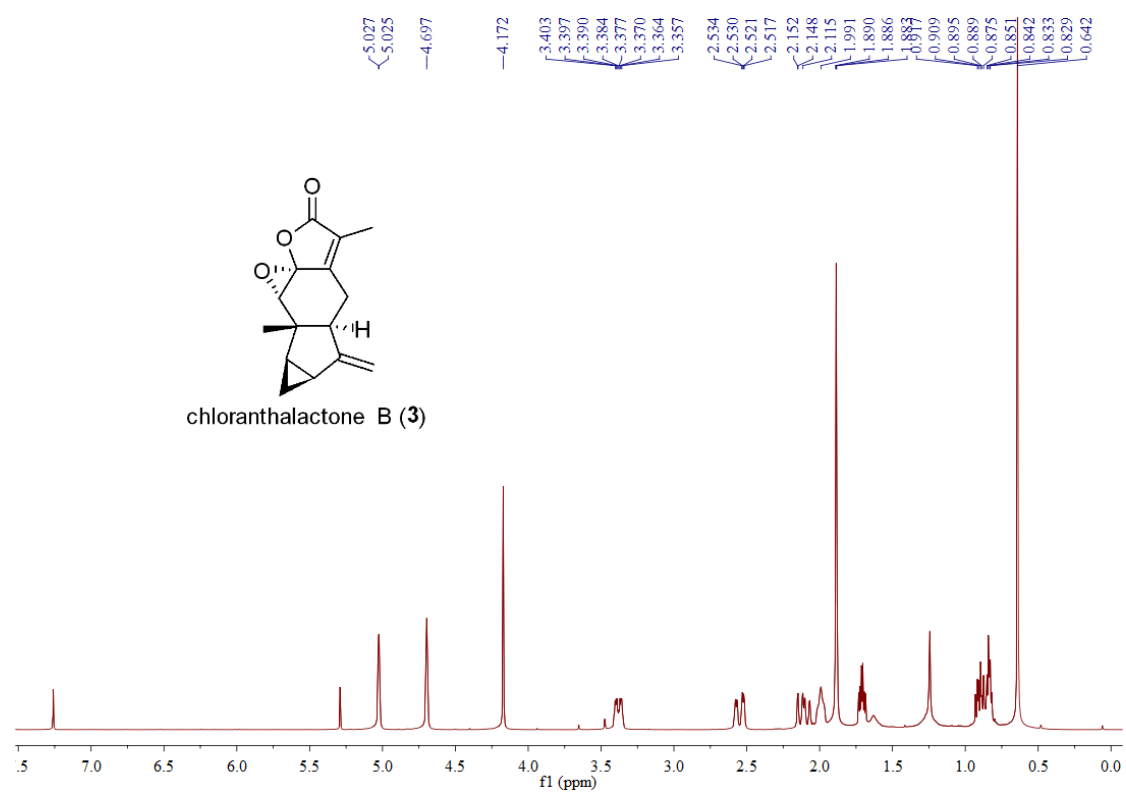
S21.  $^1\text{H}$  NMR (400 MHz,  $\text{CDCl}_3$ ) spectrum of **2**



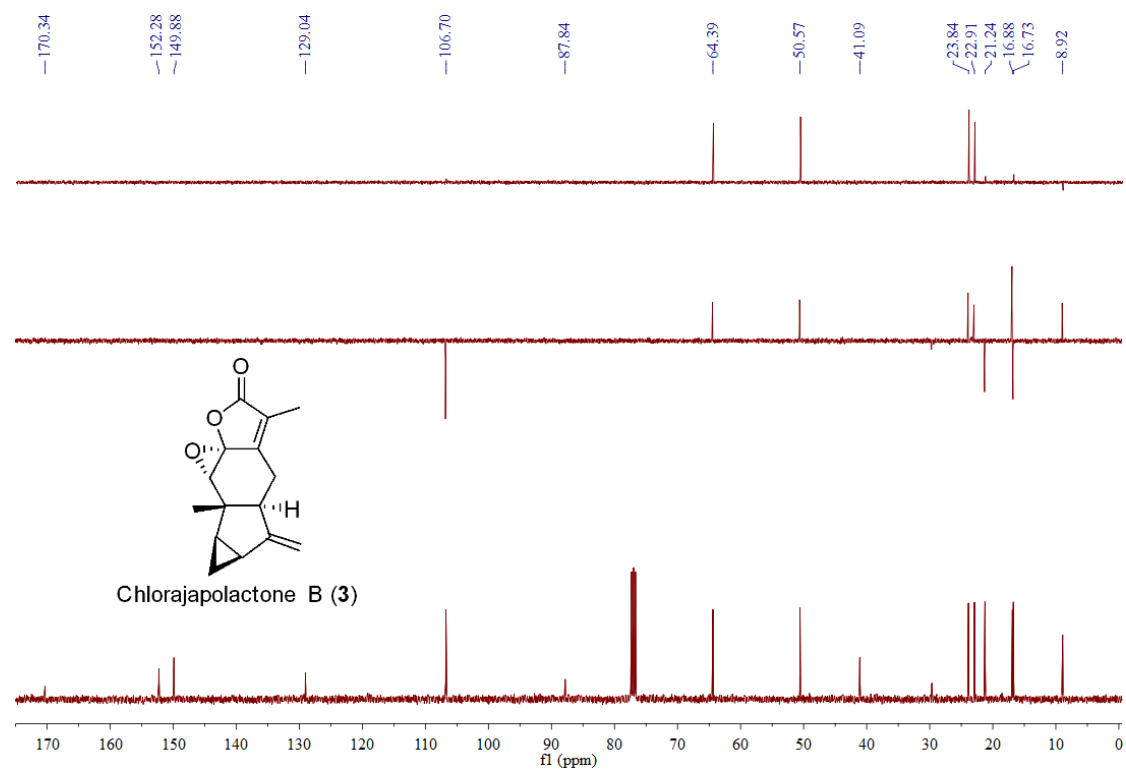
S22.  $^{13}\text{C}$  NMR (100 MHz,  $\text{CDCl}_3$ ) spectrum of **2**



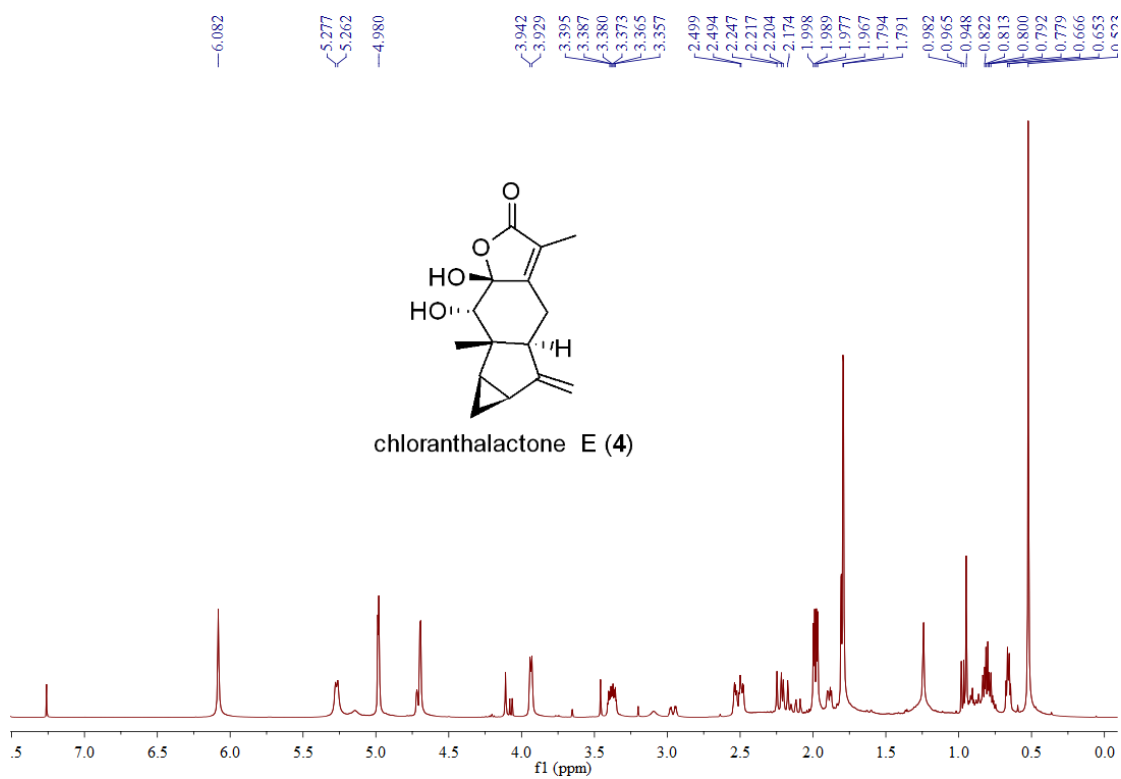
S23.  $^1\text{H}$  NMR (400 MHz,  $\text{CDCl}_3$ ) spectrum of **3**



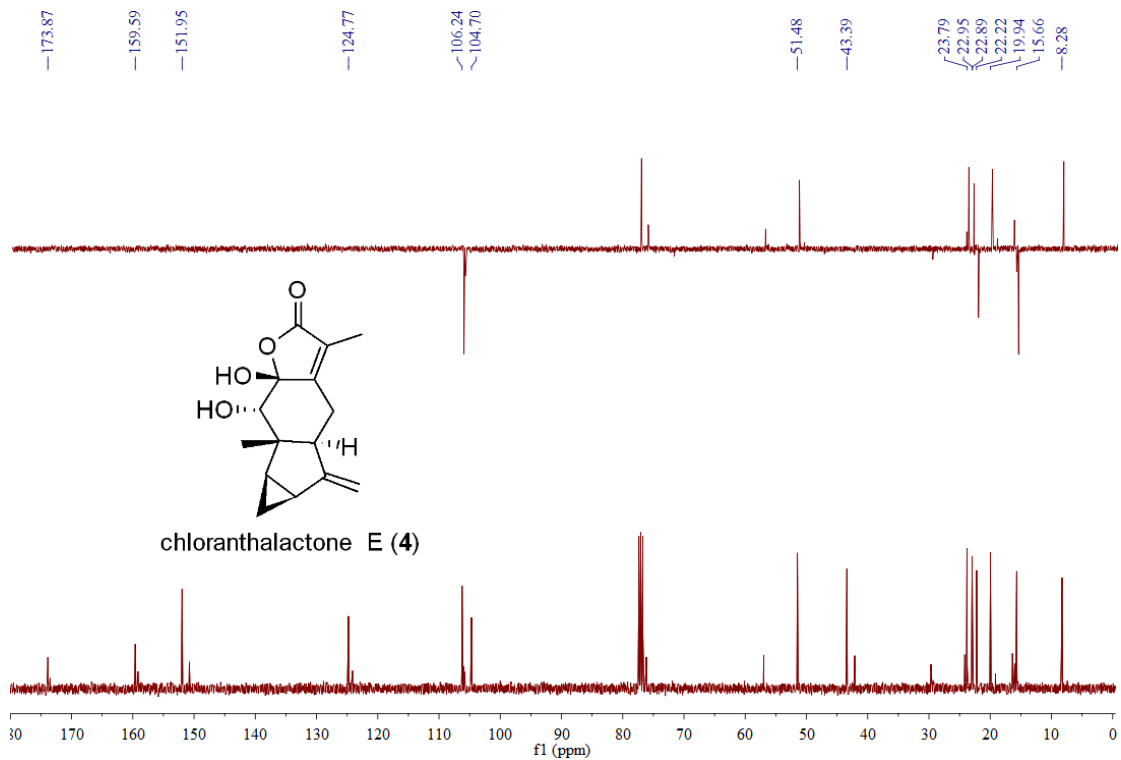
S24.  $^{13}\text{C}$  NMR (100 MHz,  $\text{CDCl}_3$ ) spectrum of **3**



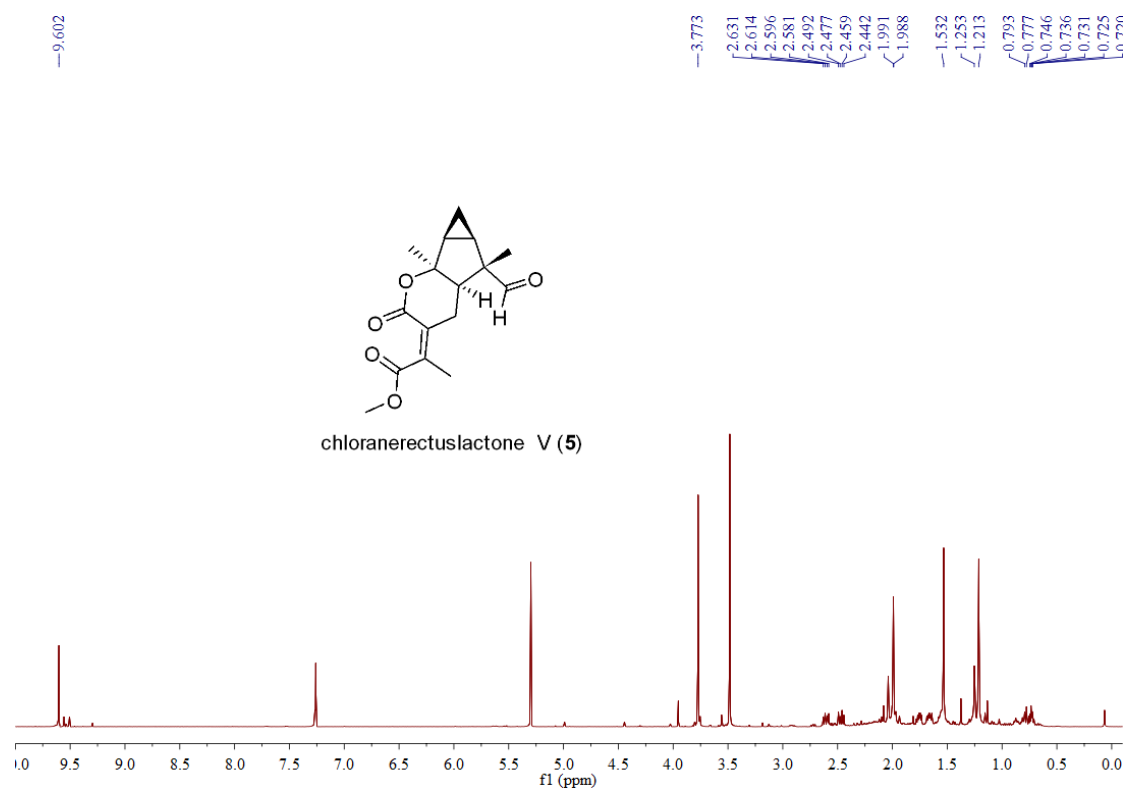
S25.  $^1\text{H}$  NMR (400 MHz,  $\text{CDCl}_3$ ) spectrum of **4**



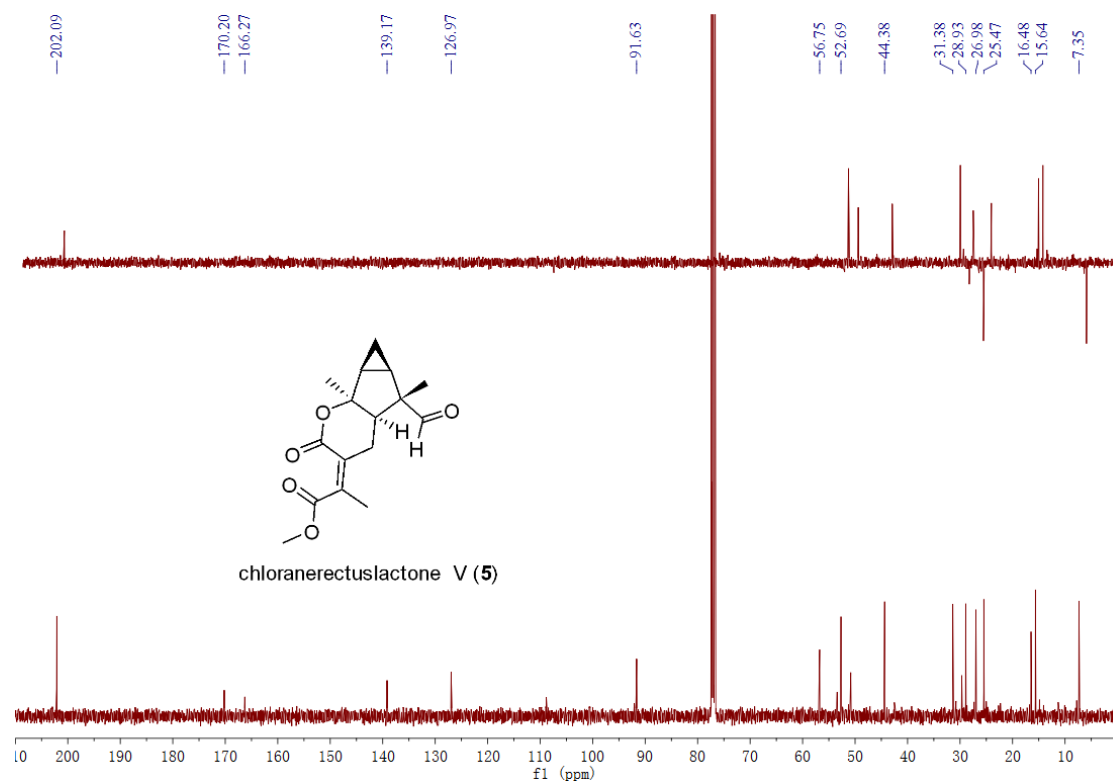
S26.  $^{13}\text{C}$  NMR (100 MHz,  $\text{CDCl}_3$ ) spectrum of **4**



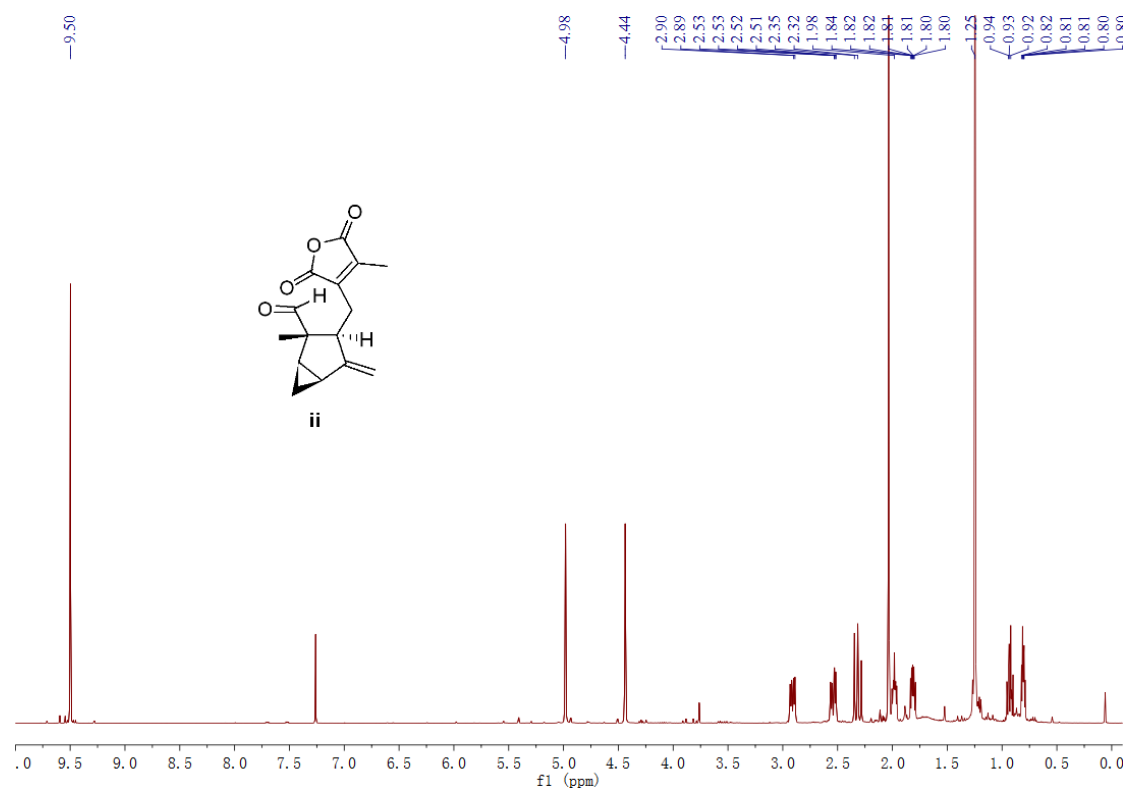
S27.  $^1\text{H}$  NMR (400 MHz,  $\text{CDCl}_3$ ) spectrum of **5**



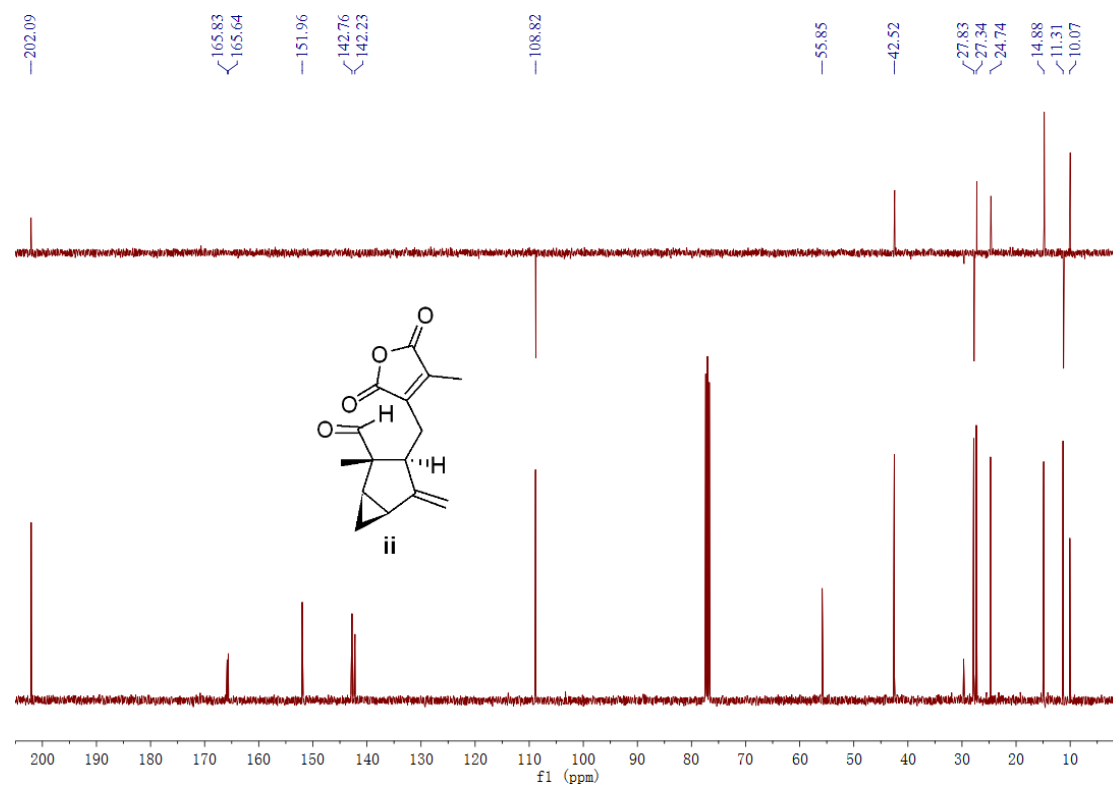
S28.  $^{13}\text{C}$  NMR (100 MHz,  $\text{CDCl}_3$ ) spectrum of **5**



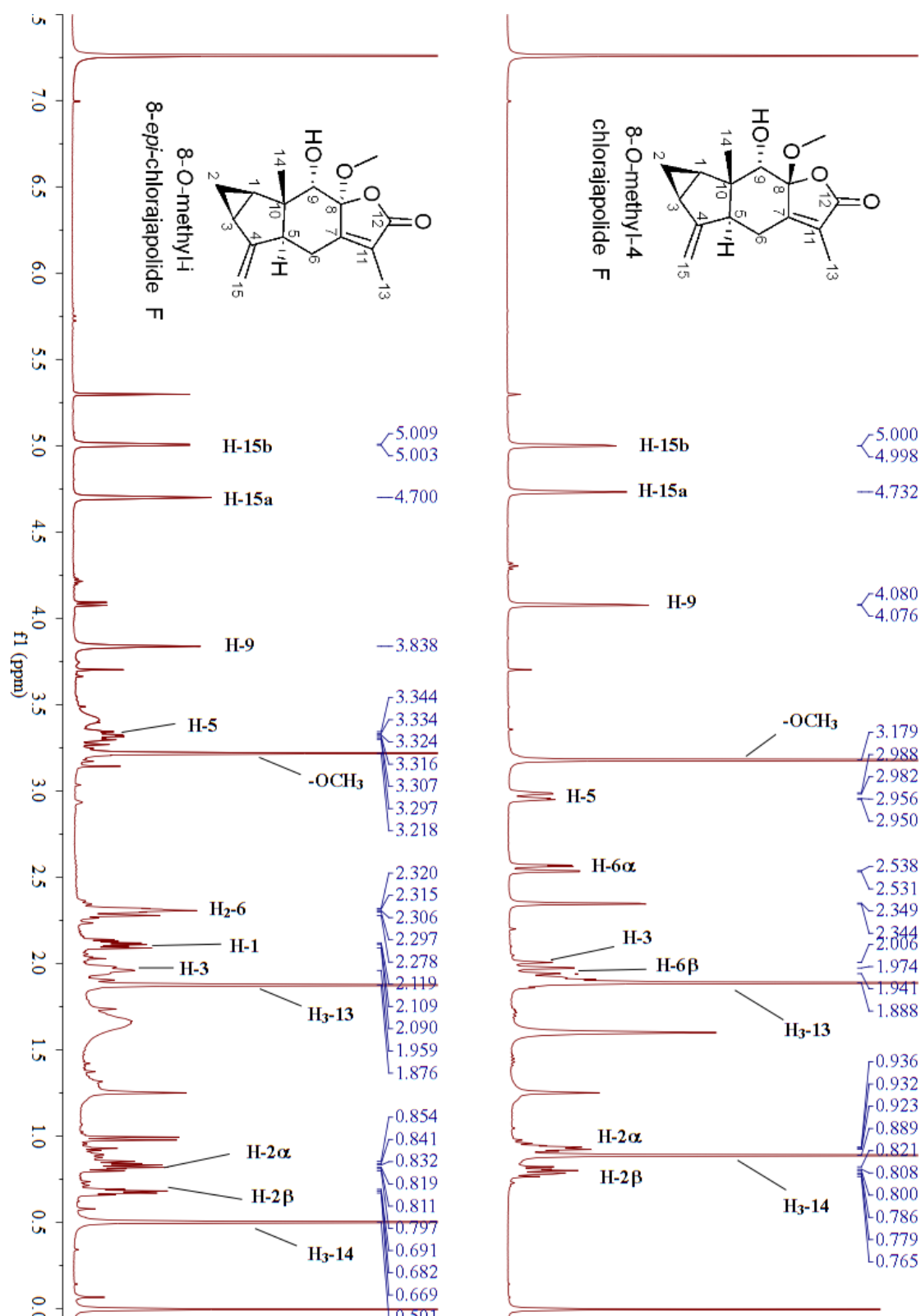
S29.  $^1\text{H}$  NMR (400 MHz,  $\text{CDCl}_3$ ) spectrum of intermediate **ii**



S30.  $^{13}\text{C}$  NMR (100 MHz,  $\text{CDCl}_3$ ) spectrum of intermediate **ii**



S31. <sup>1</sup>H NMR (400 MHz, CDCl<sub>3</sub>) spectra of **8-O-methyl-i** and **8-O-methyl-4**





S32. Chem3D Molecular Modeling Study of **1b**

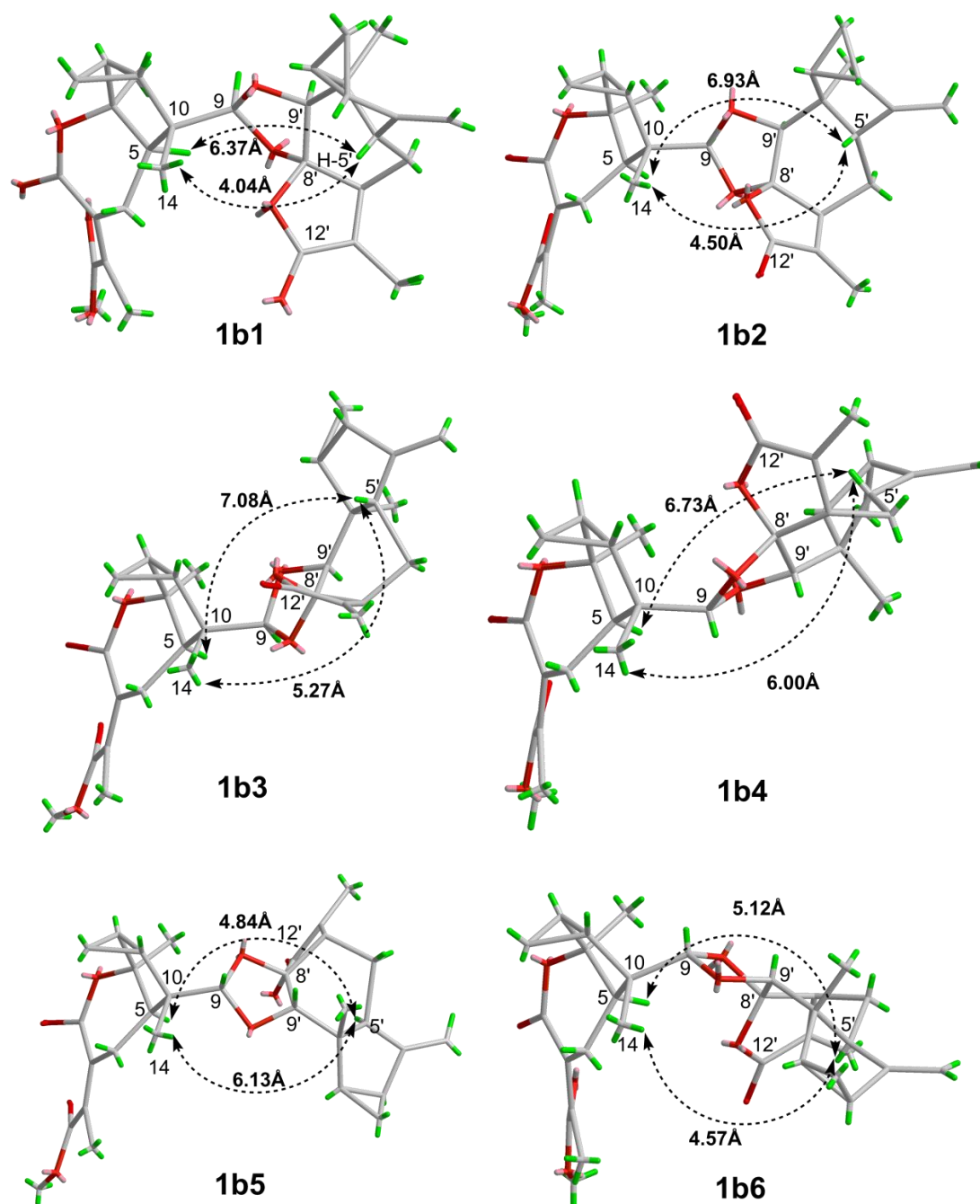


**Figure 2.** Conformers of **1b**: **1b1–1b6** represent the different conformations of **1b** rotating around C-9–C-10 bond (rotating ca. 360°). In all the cases, the distances between H-5' and H-5 or H<sub>3</sub>-14 are greater than 4 Å, which could not match the strong correlations of H-5'/H-5 and H-5'/H<sub>3</sub>-14 observed in the ROESY spectrum.

### S33. ECD spectra calculation of **1a** by TDDFT method

In general, conformational analysis was carried out via Monte Carlo searching using molecular mechanism with MMFF94 force field in the Spartan 08 program.<sup>1</sup> Due to the flexible skeleton, the results showed six possible conformers who were reoptimized using DFT at the B3LYP/6-31+G(d) level in vacuum by the Gaussian 09 program.<sup>2</sup> The B3LYP/6-31+G(d) harmonic vibrational frequencies were further calculated to confirm their stability. The energies, oscillator strengths, and rotational strengths of the first 60 electronic excitations were calculated using the TDDFT methodology at the B3LYP/6-311++G(2d,2p) level in vacuum. The ECD spectra were simulated by the overlapping Gaussian function<sup>3</sup> in which velocity rotatory strengths of the first 50 excited states were adopted. To get the final ECD spectra, the simulated spectra of the lowest energy conformers were averaged according to the Boltzmann distribution theory and their relative Gibbs free energy ( $\Delta G$ ). By comparison of the calculated ECD spectra with the experimental ones, the absolute configuration of **1** was resolved.

1. *Spartan 08*; Wavefunction Inc.:Irvine, CA.

2. *Gaussian 09*, Revision A.1, Frisch, M. J.; Trucks, G. W.; Schlegel, H. B.; Scuseria, G. E.; Robb, M. A.; Cheeseman, J. R.; Scalmani, G.; Barone, V.; Mennucci, B.; Petersson, G. A.; Nakatsuji, H.; Caricato, M.; Li, X.; Hratchian, H. P.; Izmaylov, A. F.; Bloino, J.; Zheng, G.; Sonnenberg, J. L.; Hada, M.; Ehara, M.; Toyota, K.; Fukuda, R.; Hasegawa, J.; Ishida, M.; Nakajima, T.; Honda, Y.; Kitao, O.; Nakai, H.; Vreven, T.; Montgomery, Jr., J. A.; Peralta, J. E.; Ogliaro, F.; Bearpark, M.; Heyd, J. J.; Brothers, E.; Kudin, K. N.; Staroverov, V. N.; Kobayashi, R.; Normand, J.; Raghavachari, K.; Rendell, A.; Burant, J. C.; Iyengar, S. S.; Tomasi, J.; Cossi, M.; Rega, N.; Millam, J. M.; Klene, M.; Knox, J. E.; Cross, J. B.; Bakken, V.; Adamo, C.; Jaramillo, J.; Gomperts, R.; Stratmann, R. E.; Yazyev, O.; Austin, A. J.; Cammi, R.; Pomelli, C.; Ochterski, J. W.; Martin, R. L.; Morokuma, K.; Zakrzewski, V. G.; Voth, G. A.; Salvador, P.; Dannenberg, J. J.; Dapprich, S.; Daniels, A. D.; Farkas, Ö.; Foresman, J. B.; Ortiz, J. V.; Cioslowski, J.; Fox, D. J. Gaussian, Inc., Wallingford CT, 2009.

3. Stephens, P. J.; Harada, N. ECD cotton effect approximated by the Gaussian curve and other methods. *Chirality* **2010**, *22*, 229–233.

#### 33.1. Lowest energy conformers of **1a**

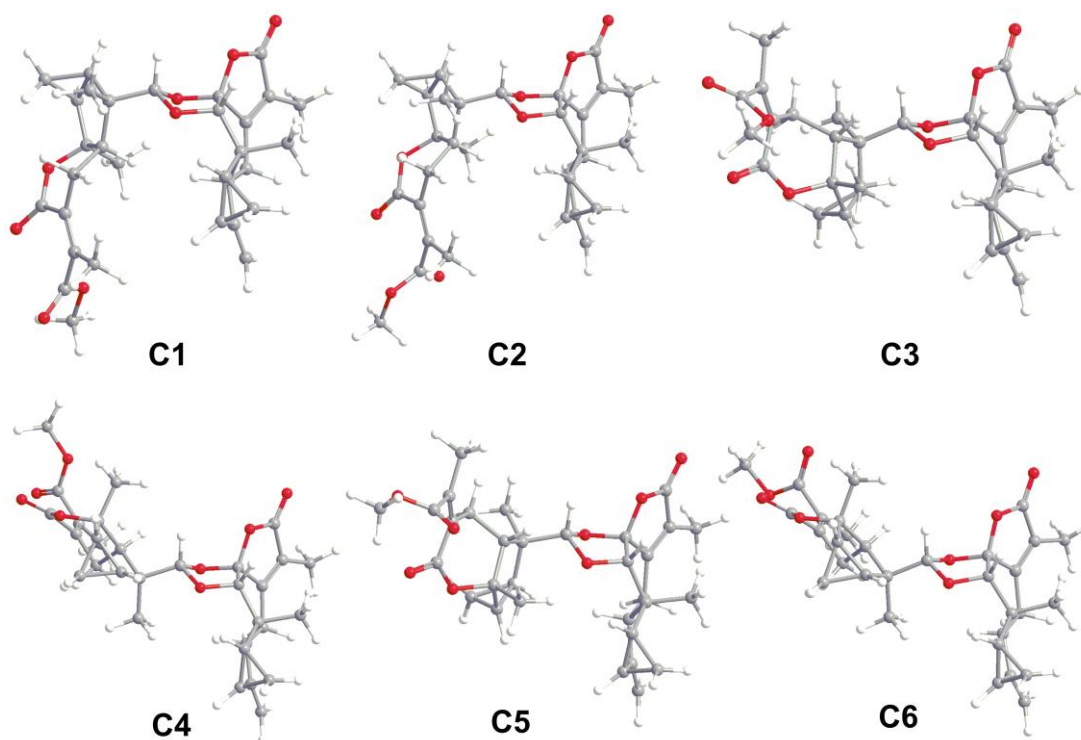


**Figure 3.** B3LYP/6-31+G(d) optimized lowest energy 3D conformers of **1**

### 33.2. Energy analysis table

conf.	Gibbs free energy (298.15 K)		
	G (Hartree)	$\Delta G$ (Kcal/mol)	Boltzmann Distribution
<b>C1</b>	-1804.182788	0.93561741	0.109
<b>C2</b>	-1804.18233	1.22301699	0.067
<b>C3</b>	-1804.182301	1.24121478	0.065
<b>C4</b>	-1804.184279	0	0.530
<b>C5</b>	-1804.181755	1.58383524	0.036
<b>C6</b>	-1804.183316	0.60429213	0.191

### 33.3. Calculated ECD data

State	<b>C1</b>		<b>C2</b>		<b>C3</b>	
	Excitation energies(eV)	Rotatory Strengths*	Excitation energies(eV)	Rotatory Strengths*	Excitation energies(eV)	Rotatory Strengths*
1	4.4378	4.5623	4.4955	0.2606	4.4404	0.4089
2	4.6217	-5.1438	4.6049	-4.0997	4.6285	-5.3521
3	4.6803	0.7517	4.6792	-0.217	4.6905	0.3585
4	4.8719	31.2815	4.9012	-0.0124	4.8709	29.9041
5	4.9667	-0.0215	5.039	25.3716	5.0566	-0.1933

State	C1		C2		C3	
	Excitation energies(eV)	Rotatory Strengths*	Excitation energies(eV)	Rotatory Strengths*	Excitation energies(eV)	Rotatory Strengths*
6	4.985	0.0819	5.076	14.598	5.1158	0.2545
7	5.2472	-1.9379	5.2542	-3.2938	5.291	-5.9215
8	5.2721	-1.4177	5.3361	-0.6923	5.3426	-4.908
9	5.481	24.1935	5.5589	-27.0091	5.4919	-15.181
10	5.5698	-25.8331	5.5924	5.448	5.6029	-88.8205
11	5.603	16.2353	5.6667	10.3826	5.6532	59.9809
12	5.6715	2.346	5.6946	-1.2885	5.7099	9.5466
13	5.7061	21.552	5.7122	2.2319	5.7177	-0.5955
14	5.7076	0.7457	5.7389	-6.2242	5.7255	8.0397
15	5.7361	3.5723	5.7483	1.6696	5.7695	-1.4281
16	5.7919	-49.4741	5.7717	-4.0025	5.7777	-1.4151
17	5.8293	1.7961	5.8285	3.6283	5.856	-10.9198
18	5.8738	6.2723	5.8458	-11.1765	5.8736	4.5954
19	5.8844	4.2438	5.8971	-15.0624	5.9078	1.3477
20	5.9495	12.2568	5.9082	2.0223	5.9697	-6.724
21	5.9565	-10.161	5.9413	1.0562	5.9709	11.2515
22	5.9646	-1.6354	5.9872	4.1886	6.002	-0.704
23	5.9902	-4.8691	6.0518	-1.4993	6.0254	-7.7367
24	6.0192	-3.59	6.0606	0.6618	6.0561	6.9059
25	6.0307	2.3233	6.0835	-0.9664	6.09	-50.8349
26	6.0937	-1.4369	6.1172	5.4749	6.1243	-4.6887
27	6.0988	-31.5432	6.1345	-12.1185	6.1432	-5.3247
28	6.1304	-8.896	6.1901	0.0235	6.1646	0.3071
29	6.1905	-0.8531	6.242	-35.7837	6.1725	-0.2498
30	6.2236	1.3333	6.2555	22.6825	6.2159	-7.3229
31	6.2422	-5.3386	6.2853	-1.0573	6.2275	-3.8216
32	6.2617	-8.137	6.2862	-3.5648	6.2865	-0.9227
33	6.2808	-7.9472	6.301	11.3907	6.2908	-5.5133
34	6.3093	0.0526	6.3071	2.1868	6.3133	7.5508
35	6.3242	6.7503	6.3325	16.8718	6.343	8.9879
36	6.3541	-5.4601	6.3492	17.1999	6.3984	4.9799
37	6.3851	7.4777	6.3734	-53.7758	6.4067	7.3617
38	6.3939	-4.46	6.4323	8.2323	6.4269	0.2866
39	6.4225	15.0202	6.4452	-5.6063	6.4419	-0.1507

State	C1		C2		C3	
	Excitation energies(eV)	Rotatory Strengths*	Excitation energies(eV)	Rotatory Strengths*	Excitation energies(eV)	Rotatory Strengths*
40	6.4363	0.0132	6.453	63.7641	6.4891	8.7782
41	6.4545	72.7902	6.4646	10.8362	6.4953	45.409
42	6.4974	-4.0454	6.4962	0.1491	6.5045	38.311
43	6.5267	27.6324	6.5152	-5.6795	6.5189	-0.0189
44	6.5693	4.2823	6.5278	39.4231	6.5386	1.6899
45	6.5718	9.9477	6.5304	-0.4428	6.5634	-6.7025
46	6.5897	-2.5084	6.5319	0.9974	6.5998	6.8596
47	6.5965	-0.648	6.5721	3.3655	6.6563	-1.3831
48	6.6018	4.9524	6.5862	-3.3824	6.6727	-9.4775
49	6.6417	0.2961	6.6617	-2.6497	6.6882	7.8935
50	6.6464	-2.2915	6.6642	-10.3954	6.6903	13.1861
51	6.6675	1.3533	6.6698	0.6122	6.695	6.1295
52	6.6703	0.8947	6.6841	0.5017	6.6965	7.8008
53	6.7175	0.516	6.6979	-6.5809	6.7099	0.7601
54	6.7251	-1.3702	6.6996	0.091	6.7253	-5.1355
55	6.7457	-2.002	6.7207	-4.713	6.7428	3.9465
56	6.7706	-45.1071	6.7375	-0.5818	6.7619	-43.5371
57	6.7824	2.0557	6.7408	-2.272	6.7793	2.042
58	6.7952	-1.4665	6.7482	3.7466	6.7968	7.5088
59	6.7987	-16.1446	6.7532	-2.6185	6.8073	-5.5555
60	6.8283	-7.0776	6.7683	-3.1396	6.813	-8.2353

\* R(velocity) 10<sup>-40</sup> erg-esu-cm

State	C4		C5		C6	
	Excitation energies(eV)	Rotatory Strengths*	Excitation energies(eV)	Rotatory Strengths*	Excitation energies(eV)	Rotatory Strengths*
1	4.4526	1.0632	4.496	-4.9848	4.5055	-4.5156
2	4.6071	-3.9804	4.62	-4.614	4.6238	-5.2766
3	4.6838	-1.5728	4.6892	-0.3483	4.6822	-0.3628
4	4.8704	30.6755	4.9647	1.1892	4.881	0.5747
5	4.9684	0.6115	5.0502	30.1334	5.0385	39.1067
6	5.1395	0.1551	5.2191	0.1365	5.2526	-3.4146
7	5.2426	4.1808	5.2847	-4.2551	5.2624	-0.1239
8	5.2695	-2.509	5.3886	-3.3467	5.3281	1.0001

State	C4		C5		C6	
	Excitation energies(eV)	Rotatory Strengths*	Excitation energies(eV)	Rotatory Strengths*	Excitation energies(eV)	Rotatory Strengths*
9	5.5106	56.8257	5.5975	46.8364	5.5958	68.4287
10	5.591	30.3108	5.609	-95.8982	5.6305	-15.6679
11	5.6406	-60.552	5.6777	-3.7958	5.6519	-0.4204
12	5.6723	0.3116	5.7005	3.8796	5.6714	-21.293
13	5.6744	3.4824	5.705	7.941	5.6885	10.8597
14	5.7304	20.6565	5.75	-22.1742	5.7432	-34.1937
15	5.7349	-86.741	5.7738	0.7073	5.7592	1.0218
16	5.7674	14.5497	5.8005	-4.8232	5.7878	-25.2191
17	5.8378	-7.749	5.8502	-2.1073	5.8569	-33.2031
18	5.862	6.5007	5.8754	-17.3018	5.8831	-6.5575
19	5.9398	-1.8403	5.967	9.426	5.9581	-1.2981
20	5.9615	0.8575	5.9736	-2.0714	5.9668	3.095
21	6.0006	-1.1864	5.9885	1.9715	5.9759	8.1104
22	6.0079	-4.3598	6.0084	0.1977	6.0015	-1.3326
23	6.0475	1.7253	6.0332	2.391	6.0406	-1.1743
24	6.065	-40.0763	6.0595	-0.7929	6.0824	-8.7153
25	6.0696	-7.9667	6.1101	-0.1509	6.1023	-17.4255
26	6.0973	-6.5535	6.1227	0.6745	6.133	-2.311
27	6.1399	-3.951	6.1393	-19.3468	6.1664	-2.3929
28	6.1961	-3.5978	6.1445	-3.3253	6.1811	-3.9347
29	6.2135	-0.0079	6.2424	-5.4817	6.215	3.0567
30	6.2551	-0.7295	6.2523	-3.5109	6.2905	-0.0722
31	6.2692	-6.615	6.2603	-1.2641	6.3005	-0.4977
32	6.2993	-4.6337	6.2693	-0.5162	6.3153	-0.7421
33	6.3246	17.8909	6.3296	11.1325	6.3334	0.0591
34	6.3293	-19.6564	6.3499	-0.1036	6.3372	-28.1035
35	6.3479	2.6687	6.3584	1.1668	6.3547	6.5615
36	6.3852	-12.9622	6.3777	-7.2907	6.3782	12.9553
37	6.3941	29.9275	6.4014	6.6305	6.4028	2.0779
38	6.4062	2.7544	6.4578	2.237	6.4208	16.7736
39	6.4339	-1.7147	6.4794	3.7867	6.4591	43.5702
40	6.4622	84.355	6.4844	65.0171	6.4629	28.6532
41	6.4678	-0.3477	6.4988	12.956	6.4779	-9.8678
42	6.5232	0.1717	6.5058	-3.4412	6.5149	-0.6473

State	C4		C5		C6	
	Excitation energies(eV)	Rotatory Strengths*	Excitation energies(eV)	Rotatory Strengths*	Excitation energies(eV)	Rotatory Strengths*
43	6.5293	-11.487	6.5315	-2.0284	6.5159	-13.3027
44	6.5578	3.4637	6.5609	-5.1522	6.5447	6.7941
45	6.5608	7.0107	6.5653	-2.2419	6.5532	4.2244
46	6.5889	6.0931	6.5956	0.9117	6.5678	-1.795
47	6.5996	6.6729	6.6107	0.1625	6.5836	21.3162
48	6.6279	2.1647	6.6408	-3.0565	6.6237	-6.5769
49	6.6543	-1.4052	6.6442	-2.7076	6.6451	-1.0301
50	6.6695	3.5307	6.6588	-31.7352	6.6651	-0.8586
51	6.69	0.1006	6.6755	-6.9502	6.6711	-1.2978
52	6.7005	5.0754	6.6784	33.1212	6.6764	3.1096
53	6.7154	0.6768	6.6903	21.9081	6.6889	-10.3647
54	6.7192	5.969	6.7084	-2.6958	6.6963	-1.743
55	6.7218	-5.3271	6.724	-1.6384	6.6999	-11.251
56	6.7603	-33.4687	6.7377	0.2751	6.7468	-0.7114
57	6.7947	7.4124	6.7687	0.7265	6.7714	-3.2869
58	6.7956	-21.5106	6.7749	-2.6818	6.7748	-4.9201
59	6.7998	-4.1506	6.788	3.9873	6.787	-0.5936
60	6.822	-0.9374	6.7914	-0.7851	6.7967	-0.8809

\* R(velocity)  $10^{**40}$  erg-esu-cm

# S34. The HRESIMS data of chlojapolactone A (1)

Formula Predictor Report - SKW-14P.lcd

Page 1 of 1

Data File: F:\尹胜\SKW-14P.lcd

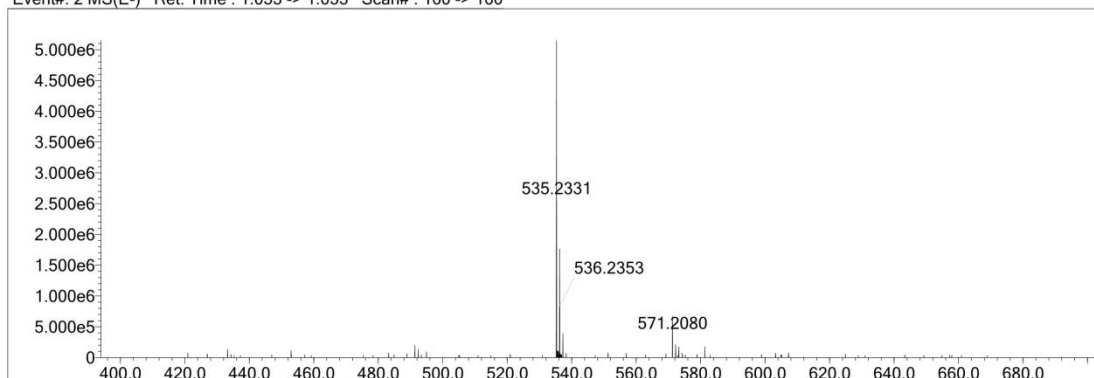
Elmt	Val.	Min	Max	Elmt	Val.	Min	Max	Elmt	Val.	Min	Max	Elmt	Val.	Min	Max	Use Adduct
H	1	10	50	N	3	0	0	P	3	0	0	Se	2	0	0	H
2H	1	0	0	O	2	5	20	S	2	0	0	Br	1	0	0	
B	3	0	0	F	1	0	0	Cl	1	0	0	I	3	0	0	
C	4	10	50	Si	4	0	0	Cu	2	0	0	10B	3	0	0	

Error Margin (mDa): 5.0  
 HC Ratio: unlimited  
 Max Isotopes: all  
 MSn Iso RI (%): 75.00

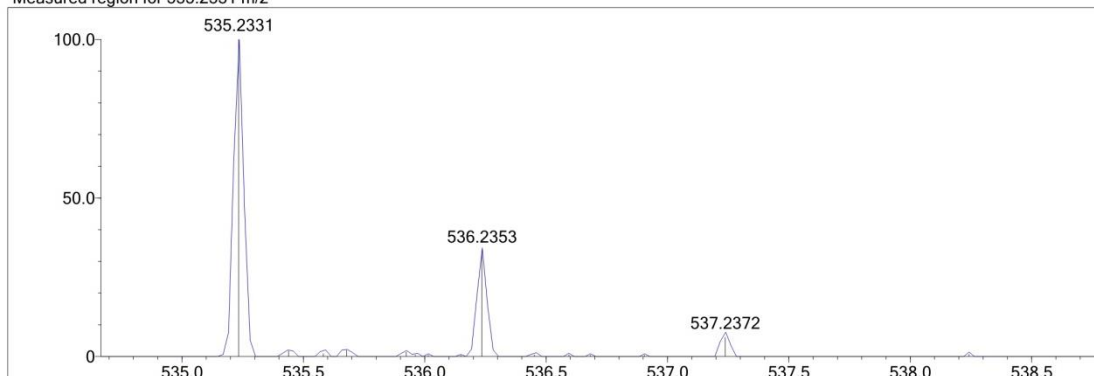
DBE Range: -2.0 - 1000.0  
 Apply N Rule: yes  
 Isotope RI (%): 1.00  
 MSn Logic Mode: AND

Electron Ions: both  
 Use MSn Info: yes  
 Isotope Res: 10000  
 Max Results: 800

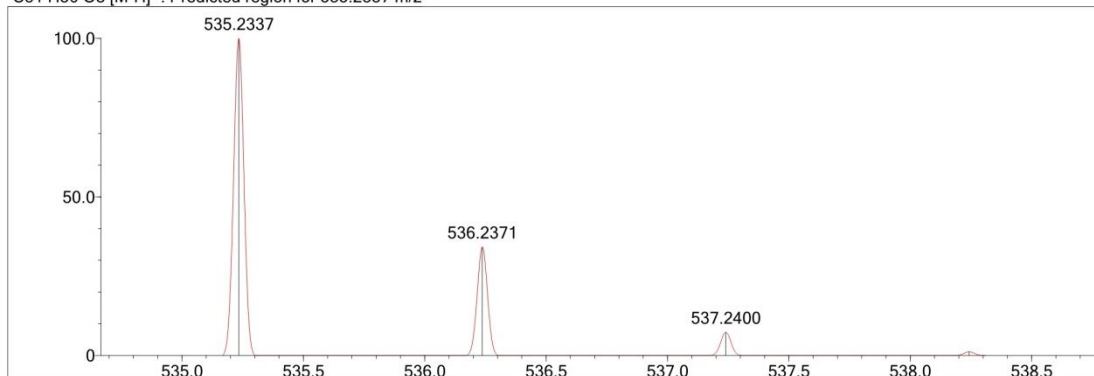
Event#: 2 MS(E-) Ret. Time : 1.053 -> 1.053 Scan#: 160 -> 160



Measured region for 535.2331 m/z



C31 H36 O8 [M-H]- : Predicted region for 535.2337 m/z



Rank	Score	Formula (M)	Ion	Meas. m/z	Pred. m/z	Df. (mDa)	Df. (ppm)	Iso	DBE
1	99.70	C31 H36 O8	[M-H]-	535.2331	535.2337	-0.6	-1.12	100.00	14.0